Carderock Division, Naval Surface Warfare Center

Bethesda, Maryland 20084-5000

NSWCCD-TR-96/006 March 1996

Survivability, Structures and Materials Directorate
Research and Development Report

Reflected-Afterflow Virtual-Source (RAVS) Model Response Compared to Exact Calculations for Elastic Cylinders Attacked by Planar Waves

by
George V. Waldo, Jr.

NSWCCD-TR-96/006 Reflected-Afterflow Virtual-Source (RAVS) Model Response Compared to Exact Calculations for Elastic Cylinders Attacked by Planar Waves

UNCLASSIFIED

SECURITY CLASSIFICATION OF THIS PAGE

REPORT DOCUMENTATION PAGE

Form Approved OMB No. 0704-0188

1a. REPORT SECURITY CLASSIFICATION: UNCLASSIFIED	1b. RESTRICTIVE MARKINGS
2a. SECURITY CLASSIFICATION AUTHORITY	3. DISTRIBUTION/AVAILABILITY OF REPORT: Approved for public release; distribution is unlimited.
2b. DECLASSIFICATION/DOWNGRADING SCHEDULE	
4. PERFORMING ORGANIZATION REPORT NUMBER(S): NSWCCD-TR-96/006	5. MONITORING ORGANIZATION REPORT NUMBER(S)
6a. NAME OF PERFORMING ORGANIZATION: Naval Surface Warfare Center Carderock Division; 6b. OFFICE SYMBOL (If applicable): Code 672	7a. NAME OF MONITORING ORGANIZATION
6c. ADDRESS (City, State, and ZIP Code): Bethesda, MD 20084-5000	7b. ADDRESS (City, State, and ZIP Code)
8a. NAME OF FUNDING/SPONSORING ORGANIZATION: Naval Surface Warfare Center Carderock Division; 8b. OFFICE SYMBOL (If applicable): Code 011	9. PROCUREMENT INSTRUMENT IDENTIFICATION NUMBER
8c. ADDRESS (City, State, and ZIP Code)	10. SOURCE OF FUNDING NUMBERS: PROGRAM ELEMENT NO. / PROJECT NO. / TASK NO / WORK UNIT ACCESSION NO.

11. TITLE (Include Security Classification)
Reflected-Afterflow Virtual-Source (RAVS) Model Response Compared to Exact Calculations for Elastic Cylinders Attacked by Planar Waves

12. PERSONAL AUTHOR(S)
Waldo, Jr., George V.

13a. TYPE OF REPORT	13b. TIME COVERED	14. DATE OF REPORT (Year, Month, Day)	15. PAGE COUNT
Final	FROM 950315 TO 950715	96 February	60

16. SUPPLEMENTARY NOTATION

17. COSATI CODES			18. SUBJECT TERMS (Continue on reverse if necessary and identify by block number)		
FIELD	GROUP	SUB-GROUP	acoustic	virtual-source	shell
			reflection	elastic	cylindrical
			afterflow	structural	approximation

19. ABSTRACT (Continue on reverse if necessary and identify by block number)

A recently developed theoretical approximation, the Reflected-Afterflow Virtual-Source (RAVS) model, is applied to the case of a planar shock wave attacking an elastic cylindrical shell. To do this, an equation of motion for a structural surface is presented. Also, equations for the pressure that develops when an acoustic wave interacts with a curved and compliant surface are presented. These equations were derived using the RAVS model. An expression for the velocity of the structural surface is derived from the equation of motion and a numerical method is developed using this expression. This is applied to the case of a planar wave attacking an elastic cylindrical shell. Calculations, using the RAVS model, are shown to be in good agreement with all of the exact calculations that were published by Huang for all locations and times. It is concluded that the RAVS model gives a good approximation for the loading and response of an elastic cylindrical shell attacked by a planar wave. The RAVS model is shown to be even better for a spherical wave

20. DISTRIBUTION/AVAILABILITY OF ABSTRACT	21. ABSTRACT SECURITY CLASSIFICATION
☐ UNCLASSIFIED/UNLIMITED ☒ SAME AS RPT. ☐ DTIC USERS	UNCLASSIFIED
22a. NAME OF RESPONSIBLE INDIVIDUAL: George V. Waldo, Jr.	22b. TELEPHONE (Include Area Code): (301) 227-1782; 22c. OFFICE SYMBOL: Code 672

DD Form 1473, JUN 86 *Previous editions are obsolete.* S/N 0102-LF-014-6603

SECURITY CLASSIFICATION OF THIS PAGE
UNCLASSIFIED

Block 19. Abstract (Continued)

attack which is a case of more practical interest.

CONTENTS

FIGURES

THIS PAGE IS INTENTIONALLY BLANK.

ABSTRACT

A recently developed theoretical approximation, the Reflected-Afterflow Virtual-Source (RAVS) model, is applied to the case of a planar shock wave attacking an elastic cylindrical shell. To do this, an equation of motion for a structural surface is presented. Also, equations for the pressure that develops when an acoustic wave interacts with a curved and compliant surface are presented. These equations were derived using the RAVS model. An expression for the velocity of the structural surface is derived from the equation of motion and a numerical method is developed for using this expression. This is applied to the case of a planar wave attacking an elastic cylindrical shell. Calculations, using the RAVS model, are shown to be in good agreement with all of the exact calculations that were published by Huang for all locations and times. It is concluded that the RAVS model gives a good approximation for the loading and response of an elastic cylindrical shell attacked by a planar wave. The RAVS model is shown to be even better for a spherical wave attack which is a case of more practical interest.

INTRODUCTION

Calculation of the deformation of a structure caused by the pressure wave from an underwater explosion is of much interest to the Navy. To gain this capability an approximate model was introduced[1,2] to determine the pressure that develops when an acoustic wave interacts with a curved and compliant surface. This model uses the virtual-source concept in analogy with geometrical optics. Because this model includes the afterflow velocities of both the attacking and reflected waves, it is called the "Reflected-Afterflow Virtual-Source" (RAVS) model. In this paper, an equation of motion for a structural surface is obtained using the RAVS model. From this equation of motion, the deformation of the surface is calculated. A computer program is

presented to determine the deformations for the special case of a planar shock wave interacting with a cylindrical elastic shell. Calculations with this program (using RAVS) are shown to be in good agreement with the exact calculations by Huang.[3,4]

EQUATION OF MOTION

The equation of motion for the velocity $u(t)$ of the surface in the direction that is *opposite* to the normal to the surface (Figure 1) is

$$m\dot{u}(t) = p_{tot}(t) - p_{str}(t) \ , \qquad \textbf{(1)}$$

where m is the total mass (including the attached stiffeners) of the structural surface per unit area, t is the time after arrival of the attacking wave, $p_{tot}(t)$ is the total pressure in the fluid, and $p_{str}(t)$ is the structural pressure, i.e., the force per unit area due to the structure in the direction that is normal to the structural surface (pointing into the fluid). This quantity is determined by the properties of the structure. The total pressure in the fluid at the point of interest on the surface of the structure is

$$p_{tot}(t) = p_{hydro} + p(t) + p_{scat}(t) + p_{rad}(t) \ , \qquad \textbf{(2)}$$

where p_{hydro} is the hydrostatic pressure, $p(t)$ is the pressure of the attacking wave, $p_{scat}(t)$ is the pressure of the scattered wave, and $p_{rad}(t)$ is the pressure of the radiated wave.

PRESSURE OF THE SCATTERED WAVE

Because the scattered wave is defined to be the wave that would occur if the surface did not move (if there were no

separation of the fluid from the surface), the velocities of the attacking and scattered waves in the direction of the normal to the surface must be equal, that is,

$$\left[\frac{p(t)}{\rho c} + \frac{1}{\rho r}\int_0^t p(t')\,dt'\right]\cos\theta = \left[\frac{p_{scat}(t)}{\rho c} + \frac{1}{\rho b}\int_0^t p_{scat}(t')\,dt'\right]\cos\beta\ , \tag{3}$$

which implies that (see Eq. 13 of Ref. 1) the pressure of the scattered wave is

$$p_{scat}(t) = \left[p(t) - c\left(\frac{1}{b} - \frac{1}{r}\right)e^{-\frac{ct}{b}}\int_0^t e^{\frac{ct'}{b}}\,p(t')\,dt'\right]\frac{\cos\theta}{\cos\beta}\ , \tag{4}$$

where θ (see Figure 1) is the angle of incidence of the attacking wave (i.e., the angle between the normal to the surface and the line from the source), r is the distance from the source, ρ is the mass density of the fluid, c is the speed of sound,

$$b = \sqrt{b_0^2 + 4a(a-b_0)\,[\sin(\alpha/2)]^2} \tag{5}$$

is the distance to the virtual source, and the cosine of the angle of the scattered wave β (between the radial direction of the equivalent sphere and the line to the virtual source) is

$$\cos\beta = \frac{b_0 + 2\,(a-b_0)\,[\sin(\alpha/2)]^2}{b}\ . \tag{6}$$

In these equations, the radius of the equivalent sphere at the point of interest, a, is given by

$$\frac{1}{a} = \frac{1}{2}\left(\frac{1}{a_1} + \frac{1}{a_2}\right), \tag{7}$$

where a_1 is the radius of curvature in a given direction on the actual surface and a_2 is the radius of curvature in the direction

that is perpendicular to the given direction. As easily shown, the radius of this equivalent sphere does not vary on the choice of the direction a_1. If the actual surface were a sphere, then $a_1=a_2=a$. However, if the actual surface were a cylinder, then a_2 is infinite and $a=2a_1$. Also, the distance b_0 from the surface of the equivalent sphere to this virtual source is given by

$$\frac{1}{b_0} = \frac{1}{d} + \frac{2}{a}, \quad for\ d \geq 0\ and\ a > 0, \tag{8}$$

where

$$d = \frac{r^2 + 2ra\cos\theta}{\sqrt{r^2 + a^2 + 2ra\cos\theta} + a} \tag{9}$$

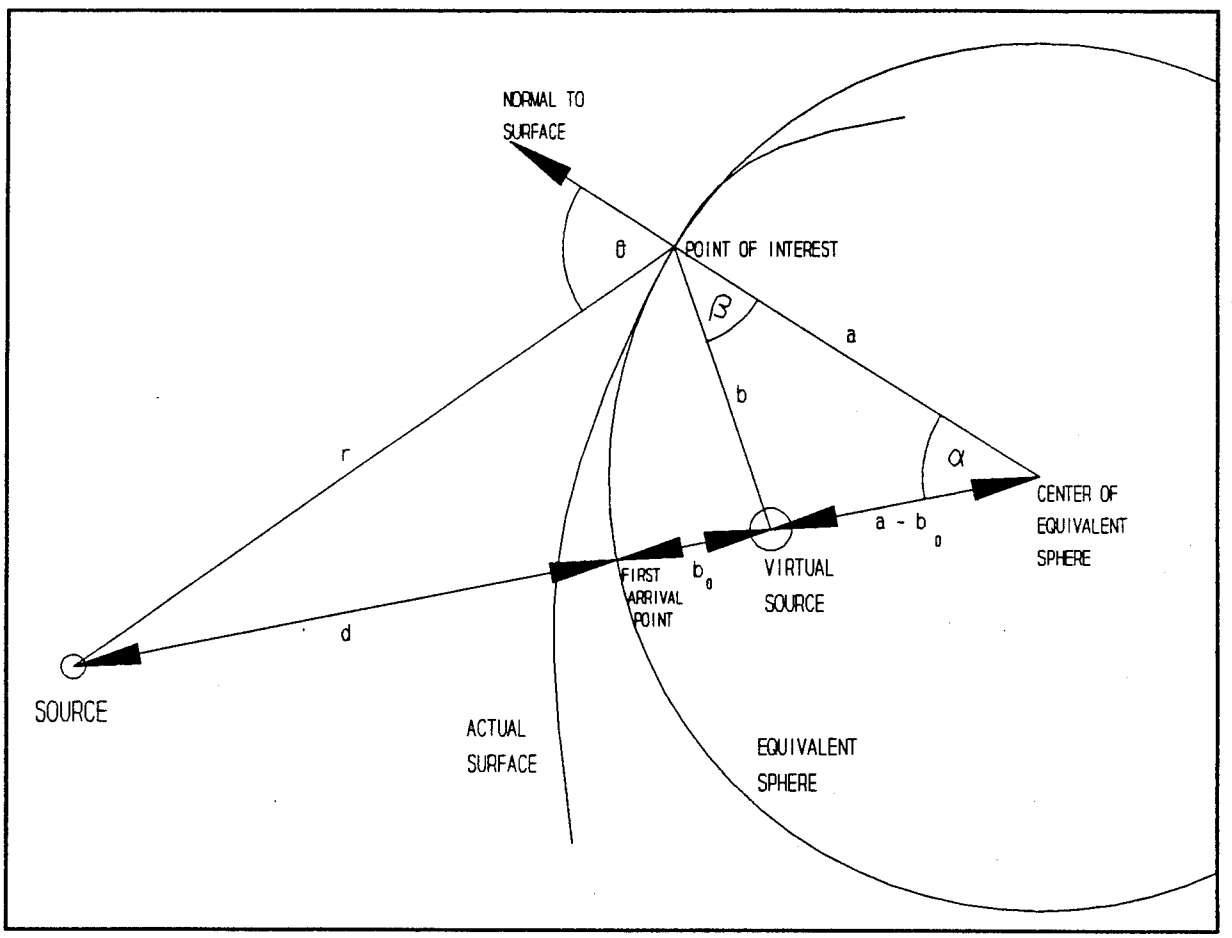

Figure 1. Geometry for virtual source.

is the distance from the source to the surface of the equivalent sphere.* The angle between the line from the source to the center of the equivalent sphere and the line from the center of the sphere to the point of interest on the structural surface is

$$\alpha = \zeta \ , \ for \ \ a + r\cos\theta \geq 0 \ , \tag{10}$$

and

$$\alpha = \zeta + \pi \ , \ \ for \ \ a + r\cos\theta < 0 \ , \tag{11}$$

where

$$\zeta = atan\left(\frac{r\sin\theta}{a + r\cos\theta}\right) \ . \tag{12}$$

PRESSURE OF THE RADIATED WAVE

The pressure at the point of interest due to the radiated wave also is modeled as if it were emanating from the virtual source. This pressure is determined by solving

$$u(t) = -\left[\frac{p_{rad}(t)}{\rho c} + \frac{1}{\rho b} \int_{-r/c}^{t} p_{rad}(t')\, dt'\right]\cos\beta \ , \tag{13}$$

where $u(t)$ is the velocity of the surface in the direction that is *opposite to* the normal to the surface, i.e., the velocity in

---

*For cases with $d < 0$, the virtual source is assumed to be located at the actual source. This implies that

$$b = r \ \ and \ \ \beta = \pi - \theta \ ,$$

see the discussion after Eq. 14 of Ref. 1.

Under certain conditions, a calculation might be acceptable for a concave surface (i.e., a surface with an equivalent sphere having a negative radius (7)). However, there are complications that could occur for other conditions. Thus, for the models that are presented in this report, it is required that $a > 0$. For numerical calculations, if a were negative, then it would have to be set equal to a very large positive number so that the effective curvature in the calculation would be approximately zero.

the direction *into* the surface of the structure. (Note that the opposite sign convention is used in Huang.[4]) Thus, the pressure of the radiated wave is

$$p_{rad}(t) = -e^{-\frac{ct}{b}} \int_{-r/c}^{t} e^{\frac{ct'}{b}} \frac{\rho c \dot{u}(t')}{\cos\beta} dt' , \tag{14}$$

as in Eq. 22 of Ref. 1.

Of course, it is *assumed* that the deformations of the surface are so small that they have a negligible effect on the curvatures. If these curvatures were continually updated during a calculation to give the current curvature, there should be an improvement in the calculation.

SOLUTION OF THE EQUATION OF MOTION

In Appendix A, it is shown that the solution of (1) is

$$u(t) = u_0(t) - u_{str}(t) , \tag{15}$$

in which the velocity, if there were no structural pressure, is

$$u_0(t) = \frac{I(t)}{m}\left(1 + \frac{\cos\theta}{\cos\beta}\right) + \frac{1}{m}\left(\frac{c}{b} + \frac{c}{r}\frac{\cos\theta}{\cos\beta}\right)\left[\frac{1}{\eta}\int_0^t p(t')\,dt' - \frac{I(t)}{\eta}\right] , \tag{16}$$

and the retarding velocity due to the structural pressure is

$$u_{str}(t) = \frac{I_{str}(t)}{m} + \frac{c}{mb}\left\{\frac{1}{\eta}\int_{-r/c}^{t} [p_{str}(t') - p_{hydro}]\,dt' - \frac{I_{str}(t)}{\eta}\right\}, \tag{17}$$

where

$$I(t) = e^{-\eta t}\int_0^t e^{\eta t'} p(t')\,dt' , \tag{18}$$

$$I_{str}(t) = e^{-\eta t} \int_{-r/c}^{t} e^{\eta t'} [p_{str}(t') - p_{hydro}] \, dt' , \tag{19}$$

and

$$\eta = \frac{c}{b} + \frac{\rho c}{m \cos\beta} \tag{20}$$

is the damping coefficient, see also (82). If $p_{str}(t)$ is not known, then it must be determined from the deformation of the structural surface.

NUMERICAL CALCULATIONS

To calculate $I(t)$ numerically (see (18)), it is useful to write

$$\begin{aligned} I(t+\Delta t) &= e^{-\eta(t+\Delta t)} \int_{0}^{t+\Delta t} e^{\eta t'} p(t') \, dt' \\ &= e^{-\eta \Delta t} I(t) + e^{-\eta(t+\Delta t)} \int_{t}^{t+\Delta t} e^{\eta t'} p(t') \, dt' . \end{aligned} \tag{21}$$

Thus, the increment of $I(t)$ is

$$\begin{aligned} \Delta I &= I(t+\Delta t) - I(t) \\ &= e^{-\eta(t+\Delta t)} \int_{t}^{t+\Delta t} e^{\eta t'} p(t') \, dt' - (1 - e^{-\eta \Delta t}) I(t) \\ &\approx e^{-\eta(t+\Delta t)} \frac{e^{\eta(t+\Delta t)} - e^{\eta t}}{\eta} p(t+\Delta t) - (1 - e^{-\eta \Delta t}) I(t) \\ &= \eta^{-1} (1 - e^{-\eta \Delta t}) p(t+\Delta t) - (1 - e^{-\eta \Delta t}) I(t) \\ &= [p(t+\Delta t) - \eta I(t)] \, Q , \end{aligned} \tag{22}$$

where

$$Q = \frac{1 - e^{-\eta \Delta t}}{\eta} = \frac{2}{\eta} \exp\left(-\frac{\eta}{2} \Delta t\right) \sinh\left(\frac{\eta}{2} \Delta t\right) . \tag{23}$$

This would be exact if $p(t)$ were constant in the interval from t

to (and including) $t+\Delta t$. Note that

$$I(t) = 0 \ , \quad for \ t \leq 0 \ . \tag{24}$$

The numerical calculation of $I_{str}(t)$ (see (19)) can be performed in a similar fashion. Thus, the increment in $I_{str}(t)$ is

$$\Delta I_{str} \approx [p_{str}(t+\Delta t) - p_{hydro} - \eta I_{str}(t)]\, Q \tag{25}$$

and

$$I_{str}(t+\Delta t) = I_{str}(t) + \Delta I_{str} \ , \tag{26}$$

where

$$I_{str}(t) = 0 \ , \quad for \ t \leq -r/c \ . \tag{27}$$

Differentiation of (17), $u_{str}(t)$, gives

$$\dot{u}_{str}(t) = \frac{\dot{I}_{str}(t)}{m} + \frac{c}{mb} I_{str}(t) \ . \tag{28}$$

Thus, the increment of $u_{str}(t)$ is

$$\Delta u_{str} \approx [\Delta I_{str} + I_{str}(t)\ (c/b)\ \Delta t]/m \tag{29}$$

and

$$u_{str}(t+\Delta t) = u_{str}(t) + \Delta u_{str} \ , \tag{30}$$

where

$$u_{str}(t) = 0 \ , \quad for \ t \leq -r/c \ . \tag{31}$$

Thus, the velocity of the surface (that is in the direction opposite to the normal to the surface) is

$$u(t) = u_0(t) - u_{str}(t) \ , \tag{32}$$

as given by (15).

EXPONENTIALLY DECAYING WAVE

Now consider an attacking pressure wave with a sudden rise and an exponential decay,

$$\begin{aligned} p(t) &= 0 , \qquad for\ t \le 0 , \\ &= p_0 e^{-qt} , \quad for\ t > 0 , \end{aligned} \tag{33}$$

where p_0 is the initial pressure and q is the exponential time-decay constant. For this case, it is convenient to define

$$s = \frac{\eta + q}{2} \tag{34}$$

and

$$\chi = \frac{\eta - q}{2} . \tag{35}$$

With these definitions (18) becomes

$$\begin{aligned} I(t) &= p_0 \frac{e^{-qt} - e^{-\eta t}}{\eta - q} = p_0 e^{-st} \frac{e^{\chi t} - e^{-\chi t}}{2\chi} \\ &= p_0 t e^{-st} sh(\chi t) , \quad for \quad t > 0 , \end{aligned} \tag{36}$$

where

$$\begin{aligned} sh(x) &= \frac{\sinh(x)}{x} , \quad for\ x \neq 0 , \\ &= 1 , \quad for\ x = 0 . \end{aligned} \tag{37}$$

Thus, the velocity if there were no structural pressure, (16), is

$$u_0(t) = \frac{I(t)}{m}\left(1 + \frac{\cos\theta}{\cos\beta}\right) + \left(\frac{c}{b} + \frac{c}{r}\frac{\cos\theta}{\cos\beta}\right)\frac{J(t)}{m} , \tag{38}$$

where, for numerical calculations,

$$J(t) = \frac{1}{\eta}\int_0^t p(t')\,dt' - \frac{I(t)}{\eta} = \frac{p_0}{\eta}\frac{1-e^{-qt}}{q} - \frac{p_0}{\eta}\frac{e^{-qt}-e^{-\eta t}}{\eta-q}$$

$$= \frac{p_0}{\eta}\frac{\eta-q-\eta e^{-qt}+qe^{-\eta t}}{q(\eta-q)} = \frac{p_0}{\eta q}\left[1+\frac{-(s+\chi)e^{-(s-\chi)t}+(s-\chi)e^{-(s+\chi)t}}{2\chi}\right]$$

$$= \frac{p_0}{\eta q}\left[1-e^{-st}\frac{(s+\chi)e^{\chi t}-(s-\chi)e^{-\chi t}}{2\chi}\right]$$

$$= \frac{p_0}{\eta q}\left\{1-e^{-st}\left[\cosh(\chi t)+s\frac{\sinh(\chi t)}{\chi}\right]\right\}$$

$$= \frac{p_0}{\eta q}\{1-e^{-st}[\cosh(\chi t)+st\,sh(\chi t)]\}\ ,\quad for\ qt>\epsilon\ and\ \eta t>\epsilon\ , \tag{39}$$

in which

$$1 >> \epsilon > 0\ ,\quad (e.g.,\ \epsilon = 0.0001)\ , \tag{40}$$

see (37) for $sh(x)$. Otherwise, for numerical calculations,

$$J(t) = p_0\frac{\frac{1-e^{-qt}}{q}-\frac{1-e^{-\eta t}}{\eta}}{\eta-q}$$

$$= \frac{p_0}{\eta-q}\left[\frac{2}{q}e^{-\frac{qt}{2}}\sinh\left(\frac{qt}{2}\right)-\frac{2}{\eta}e^{-\frac{\eta t}{2}}\sinh\left(\frac{\eta t}{2}\right)\right]$$

$$= \frac{p_0 t}{\eta-q}\left[e^{-\frac{qt}{2}}sh\left(\frac{qt}{2}\right)-e^{-\frac{\eta t}{2}}sh\left(\frac{\eta t}{2}\right)\right]\ , \tag{41}$$

$$for\ qt\le\epsilon\ and/or\ \eta t\le\epsilon\ and\ \chi^2>(\epsilon s)^2\ ,$$

otherwise, for numerical calculations,

$$J(t) = p_0\frac{t^2}{2}\ ,\quad for\ qt\le\epsilon\ and/or\ \eta t\le\epsilon\ and\ \chi^2\le(\epsilon s)^2\ . \tag{42}$$

PLANAR ATTACKING WAVE

For a planar attacking wave, the source is at an infinite distance,

$$r \to \infty \,. \tag{43}$$

In this case,

$$d \to \infty \,, \tag{44}$$

$$\alpha \to \theta \,, \tag{45}$$

and

$$b_0 \to a/2 \,, \tag{46}$$

see (8)-(12).

CYLINDRICAL STRUCTURAL SURFACE

For a cylindrical structural surface, a_2 is infinite. Thus, for a planar wave propagating perpendicular to the axes of the cylinder,

$$a = 2a_1 \;\; and \;\; b_0 = a_1 \,, \tag{47}$$

see (7) and (8). Also, the angle of incidence, θ, is the same as the angle of the point of interest on the cylinder above the direction of propagation of the wave, see Figure 2.

For a cylindrical structural surface (i.e., shell, Figure 2) composed of elastic material with Young's modulus, E, Poisson's ratio, ν, thickness, $2h$, and radius a_1, it is shown in Appendix B (see (97)) that the structural resistance pressure is

$$p_{str} = \frac{2Eh}{(1-\nu^2)a_1^2}\left[d_{radial} + \frac{h^2}{3a_1^2}d_{radial}^{(4)} - d_\theta^{(1)} + \frac{h^2}{3a_1^2}d_\theta^{(3)}\right] , \tag{48}$$

where d_{radial} is the deflection in the radial direction, d_θ is the deflection in the tangential direction, and the superscripts (in parentheses) indicate partial differentiation with respect to θ. Also, it is shown in Appendix B (see (98)) that the equation of motion for the tangential deflection is

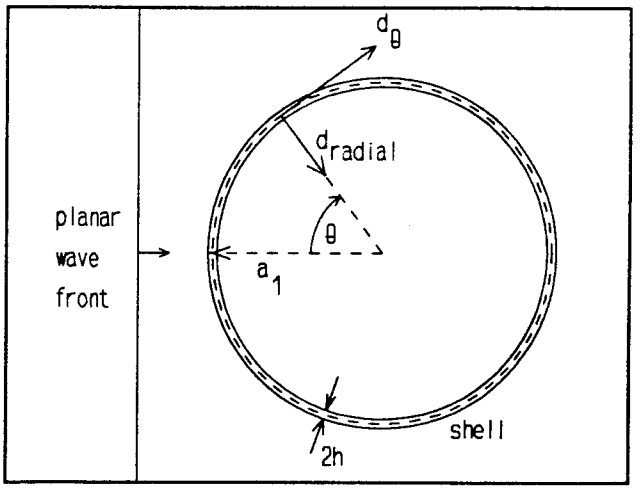

Figure 2. Planar wave attacking cylindrical shell.

$$\ddot{d}_\theta = \frac{1}{m}\frac{2Eh}{(1-\nu^2)a_1^2}\left[\left(1+\frac{h^2}{3a_1^2}\right)d_\theta^{(2)} - d_{radial}^{(1)} + \frac{h^2}{3a_1^2}d_{radial}^{(3)}\right], \qquad (49)$$

in which the mass per unit area of the shell is

$$m = 2\rho_s h, \qquad (50)$$

where ρ_s is the mass density of the shell material.

For numerical calculations, the radial deflection is approximated as

$$d_{radial}(t+\Delta t) \approx d_{radial}(t) + [u(t) + u(t+\Delta t)]\,\Delta t/2, \qquad (51)$$

using (32) for $u(t)$ and (48) for $p_{str}(t)$. Using (49), the tangential velocity is approximated as

$$\dot{d}_\theta(t+\Delta t) \approx \dot{d}_\theta(t) + \ddot{d}_\theta(t)\,\Delta t \qquad (52)$$

and the tangential deflection is

$$d_\theta(t+\Delta t) \approx d_\theta(t) + [\dot{d}_\theta(t) + \dot{d}_\theta(t+\Delta t)]\,\Delta t/2. \qquad (53)$$

A computer program (written in the *Mathematica*[5] language) using these equations is presented in Appendix C.

COMPARISONS TO EXACT CALCULATIONS

Exact calculations for this problem were performed by Huang[4] with $p_{hydro}=0$. In Eq. (1) of Huang's paper, the following dimensionless quantities are introduced:

$$M = \rho a_1/(2h\rho_s) \quad and \quad C^2 = E/[\rho_s(1-\nu^2)c^2] \ . \tag{54}$$

His results for these quantities can be regarded as functions of the number of radial transit times after arrival of the front of the attacking wave at $\theta=0$, i.e.,

$$T^* = cT/a_1 \ , \tag{55}$$

where T is the time after arrival of the attacking wave at* $\theta=0$.

In a similar fashion, the nondimensional radial velocity is defined as

$$u^* = u\frac{\rho c}{p_0} \ , \tag{56}$$

where

$$\frac{p_0}{\rho c} \tag{57}$$

is the velocity of the fluid immediately behind the front of the attacking wave (see Cole,[6] p. 35).

---

*Thus, the time after arrival of the front at a given location is

$$t = T - \frac{a_1}{c}(1-\cos\theta) \ .$$

Situation with $M=2$, $h/a_1=1/31$, and $C^2=13.685665$

The situation with $M=2$, $h/a_1=1/31$, and $C^2=13.685665$ was treated for $q=0$ and $q=c/a_1$ as follows:

1. For $q=0$, Figure 3 shows the comparison of the RAVS calculation (thin line) with Huang's exact calculation (**thick** line) for a step rise in attacking pressure with no decay (so $q=0$, see (33)). Note that the curves are very close even though the minima of the oscillations in the RAVS calculation are slightly lower than those in Huang's calculation,*

The 0-th mode of the radial displacement (see Eq. 5 of Huang[4]) is defined as

$$d_{radial0}(t) = \frac{1}{2\pi}\int_0^{2\pi} d_{radial}(t,\theta)\,d\theta$$

$$= \frac{1}{\pi}\int_0^{\pi} d_{radial}(t,\theta)\,d\theta\ , \qquad (58)$$

because of symmetry. The nondimensional form of this quantity,

*Because Huang's exact calculation contains only eight modes, it is not quite exact. However, because the convergence is very rapid, there is little error in Huang's calculation. Also, because his curves were read directly from his journal article, there are some small errors in the presentation of his curves in this paper. As can be seen in the program in Appendix C, the calculation with the RAVS model had 12 space intervals for $\theta=0$ to $\theta=\pi$. For double this number of intervals, the calculation was about the same. Thus, the calculation is sufficiently accurate for this comparison.

$$d^*_{radial0} = \frac{d_{radial0}}{a_1}\frac{\rho c^2}{p_0} , \qquad (59)$$

is plotted in Figure 4. Again, the curves are very close. Also, the RAVS calculation at 10 radial transit times, *0.1458*, is almost the same as the exact asymptotic value $M/C^2=0.1461$ (Huang[4]).

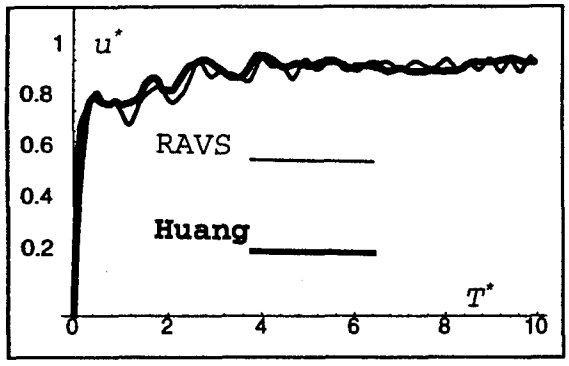

Figure 3. Nondimensional velocity vs. time, $\theta=0$, $q=0$, $M=2$.

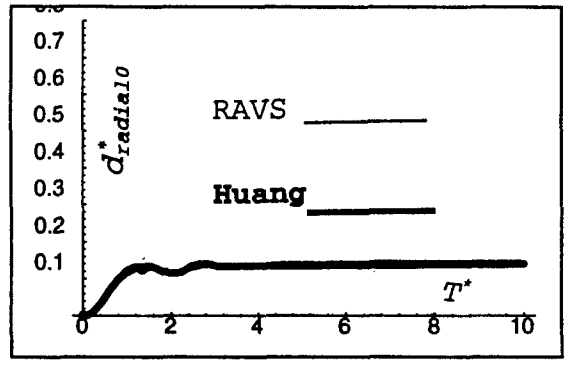

Figure 4. Nondimensional displacement, 0-th mode, $q=0$, $M=2$.

The 1-st mode of the radial velocity (see Eq. 5 of Huang[4]) is defined as

$$u_1(t) = \frac{2}{\pi}\int_0^{\pi} u(t,\theta)\cos\theta\, d\theta . \qquad (60)$$

The nondimensional form of this quantity,

$$u_1^* = u_1\frac{\rho c}{p_0} , \qquad (61)$$

is plotted in Figure 5. Again, the curves are very close.

2. For $q=c/a_1$, Figure 6 shows that the agreement is also very good for $q=c/a_1$.

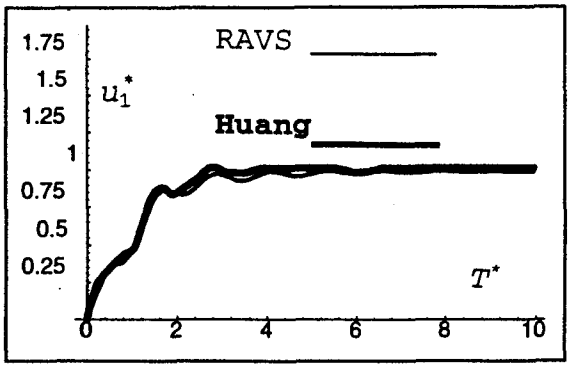

Figure 5. Nondimensional velocity vs. time, 1-st mode, *q=0, M=2.*

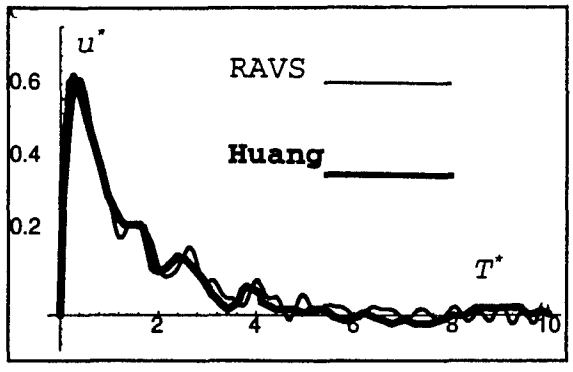

Figure 6. Nondimensional velocity vs. time, $\theta=0$, $q=c/a_1$, $M=2$.

Situation with $M=4.4189$, $h/a_1=1/69$, and $C^2=12.581197$

The situation with $M=4.4189$, $h/a_1=1/69$, and $C^2=12.581197$ was treated for $q=0$ and $q=3c/a_1$ as follows:

1. For $q=0$, Figure 7 shows that the agreement is very good where $\theta=0$. In particular, the first two (most important) oscillations are reproduced by the RAVS calculation with very little error. Also, the agreement at $\theta=\pi/2$ (Figure 8) is very good. In addition, the agreement at $\theta=\pi$ (at the back of the cylinder, see Figure 9) is very good up to two radial transit times. For later times the RAVS velocity is a fair approximation of the exact velocity even though it is somewhat lower. However, for most practical situations, the front side is of the greatest interest. For these situations, the calculation for the back of the cylinder does not need to be

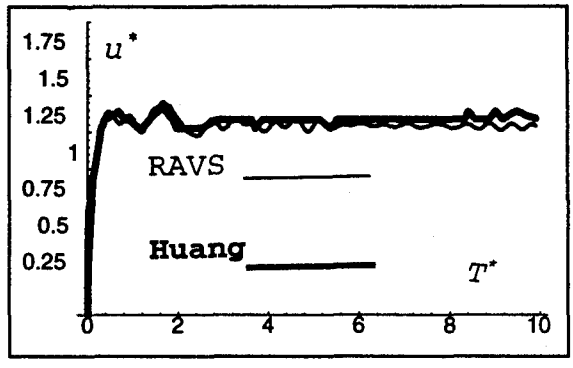

Figure 7. Nondimensional velocity vs. time, $\theta=0$, $q=0$, $M=4.4189$.

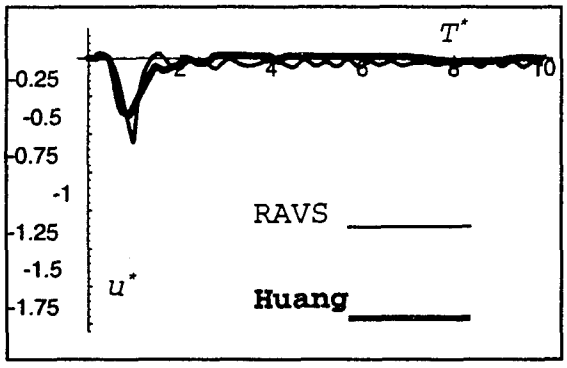

Figure 8. Nondimensional velocity vs. time, $\theta=\pi/2$, $q=0$, $M=4.4189$.

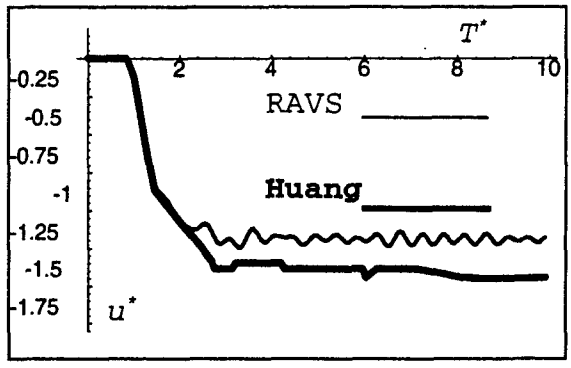

Figure 9. Nondimensional velocity vs. time, $\theta=\pi$, $q=0$, $M=4.4189$.

very accurate if it is not too large. In many practical situations, the cylinder contains enough internal equipment to make the entire object neutrally buoyant. Often, after two radial transit times, this internal equipment attains velocities that are close to the velocity of the shell. That is, the entire object moves almost as if it were a neutrally buoyant shell such as was treated in Figures 3-5. Thus, if the entire object (including internal equipment) were modeled using the RAVS model, then it is plausible that the motions would be close to those of the neutrally buoyant shell for which the agreement is very good with the exact calculations. Hence, in practical situations, the RAVS calculation might be close to the exact motion even on the back of the shell.

The exact calculation of the strains for this situation (Figures 10-12) are in very good agreement with the RAVS

calculations for all times and all locations.* Note that, in these figures, the ordinate is defined as the strain multiplied by a nondimensional factor, i.e.,

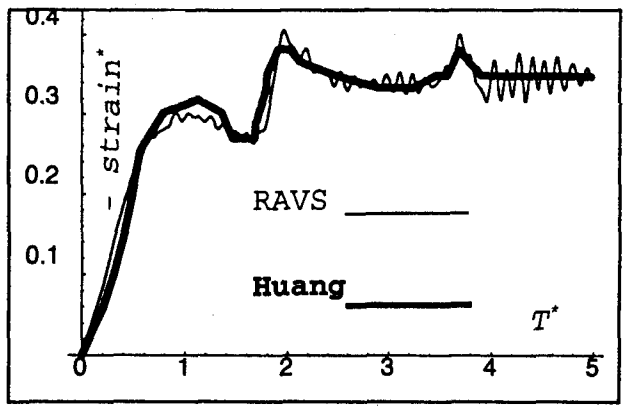

Figure 10. Strain vs. non-dimensional time $\theta=0$, $q=0$, $M=4.4189$.

$$strain^* = strain\,\frac{\rho c^2}{p_0}\ , \ where\ strain = \frac{d_\theta^{(1)} - d_{radial}}{a_1}\ . \quad (62)$$

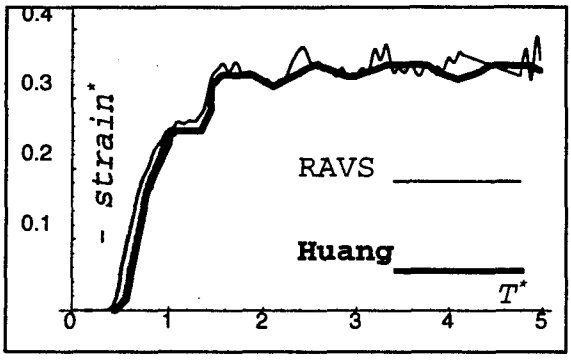

Figure 11. Strain vs. non-dimensional time, $\theta=\pi/2$, $q=0$, $M=4.4189$.

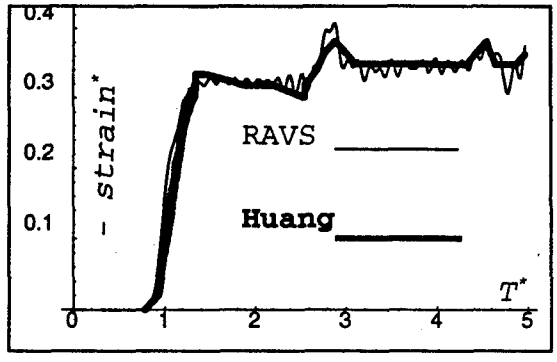

Figure 12. Strain vs. non-dimensional time, $\theta=\pi$, $q=0$, $M=4.4189$.

The most important oscillatory behavior is accurately replicated

*The small-amplitude and high-frequency oscillations are due to using only 48 intervals from $\theta=0$ to $\theta=\pi$. If more intervals were used, then these amplitudes would be even smaller and these frequencies would be even higher. This would make the agreement with the exact calculation even better.

Note that all of the calculations have only 12 intervals except the strain calculations (Figures 10-12 and Figures 15-17 which have 48 intervals) and the calculations with $q=4.8c/a_1$ (Figures 22-26 which have 24 intervals).

by the RAVS calculation. Even though the *velocity* (Figure 9) at $\theta=\pi$ was somewhat smaller than the exact calculation after two radial transit times, the *strain* (Figure 12) at this location is almost the same as the exact calculation. This is significant because the strains are a better measure of the condition of the shell than the velocity.

The 0-th mode for the radial displacement (58) is shown in Figure 13. Again the agreement is very good. At 10 radial transit times, the RAVS calculation is *0.35111* which is almost the same as the exact asymptotic value (Huang[4]), $M/C^2=0.35123$. As expected, the 0-th mode of displacement is almost the same as the values of strain for this time.

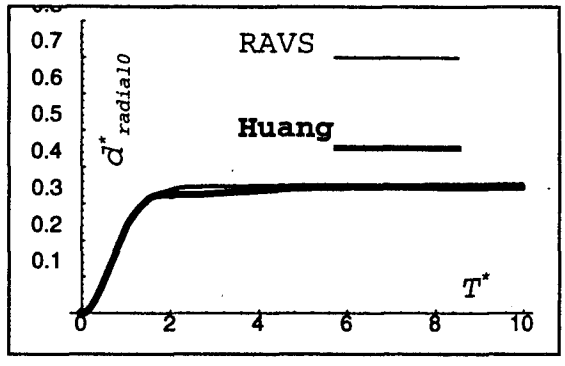

Figure 13. Nondimensional displacement, 0-th mode, *q=0, M=4.4189.*

The exact values of the 1-th mode for velocity (Figure 14) are almost the same as the values calculated using the RAVS model up to two radial transit times. For later times, the RAVS model gives a good approximation even though the values are somewhat lower. These lower values are due to the lower values of velocity at the back of the cylinder.

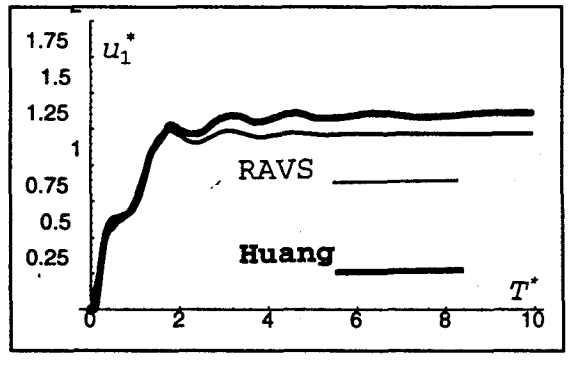

Figure 14. Nondimensional velocity vs. time, 1-st mode, *q=0, M=4.4189.*

2. For $q=3c/a_1$, Figures 15-17 show that the agreement for all locations and times is also very good. As in the previous case, the oscillations are also accurately calculated by using the RAVS method.

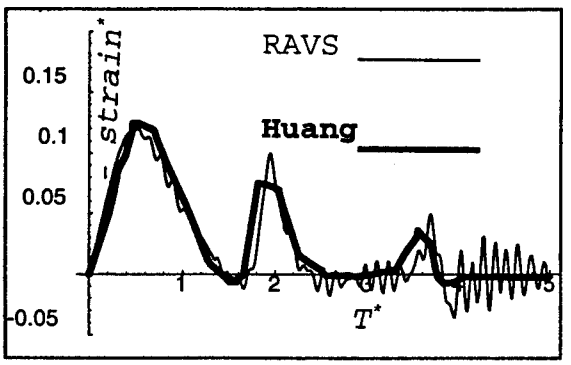

Figure 15. Strain vs. non-dimensional time, $\theta=0$, $q=3c/a_1$, $M=4.4189$.

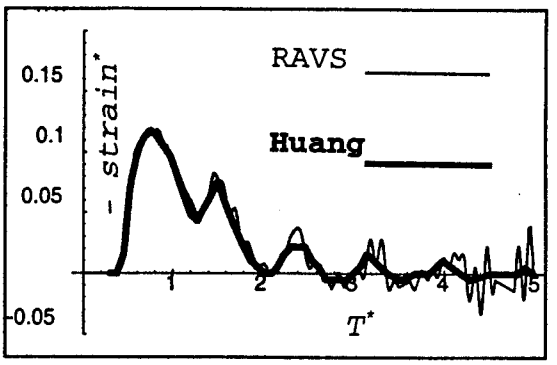

Figure 16. Strain vs. non-dimensional time, $\theta=\pi/2$, $q=3c/a_1$, $M=4.4189$.

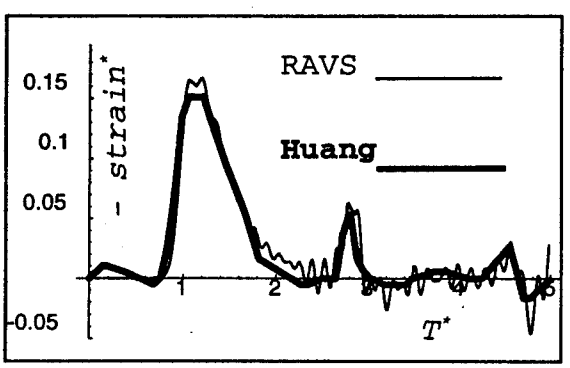

Figure 17. Strain vs.non-dimensional time, $\theta=\pi$, $q=3c/a_1$, $M=4.4189$.

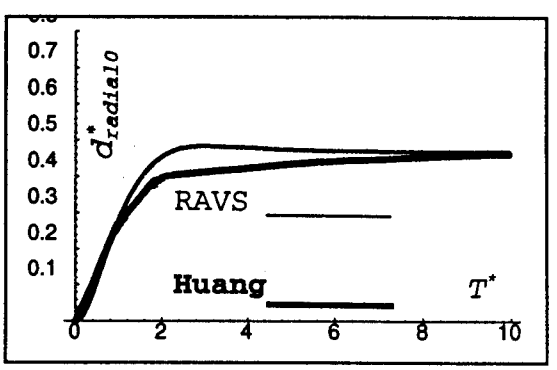

Figure 18. Nondimensional displacement, 0-th mode, $q=0$, $M=6.41975$.

Situation with $M=6.41975$, $h/a_1=1/100$, $C^2=13.685665$, and $q=0$

The situation with $M=6.41975$, $h/a_1=1/100$, $C^2=13.685665$, and $q=0$, is compared for the 0-th displacement mode in Figure 18. Even though the RAVS calculation rises somewhat faster than the exact calculation, the agreement is very good. The value for 10 radial transit times is *0.46909* which is the same as the exact asymptotic value (Huang[4]), $M/C^2=0.46909$, to five significant

figures. The RAVS calculation of the 1-st velocity mode, Figure 19, agrees very well up to two radial transit times. At later times, it is a fair approximation even though it is lower than the exact values. Unfortunately, Huang[4] did not present the calculations for the velocities and strains at individual locations for this situation. As previously explained, for many situations of interest with internal equipment inside the shell, the velocities at later times would tend to be the same as in the neutrally buoyant situation. For the neutrally buoyant situation, the RAVS calculation agrees very well with the exact calculation. Thus, the small deviation after two radial transit times might be of little practical interest. Also, in the previous situation, the velocities on the front of the cylinder and the strains at all locations were very close to the exact calculations, even though the 0-th velocity mode was somewhat lower than the exact calculation after two radial transit times. Thus, it is plausible that the velocities on the front of the cylinder and the strains at all locations are in better agreement than the 1-st velocity mode.

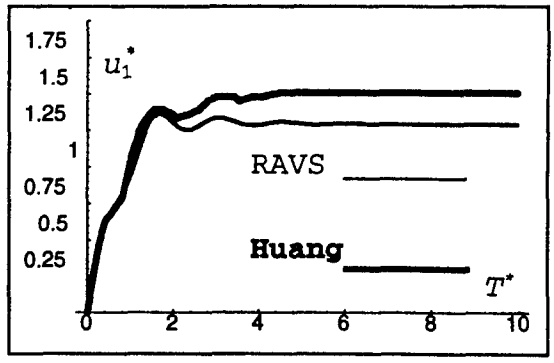

Figure 19. Nondimensional velocity vs. time, 1-st mode, *q=0, M=6.41975.*

Situation with M=9.09184, h/a_1=1/142, C^2=12.581197, and q=0

Similar remarks apply to the situation with *M=9.09184, h/a_1=1/142, C^2=12.581197, and q=0*, which is presented in Figures

20 and 21. In Figure 20, the value for 10 radial transit times is *0.7213* which is almost the same as the exact asymptotic value (Huang[4]), $M/C^2=0.7227$.

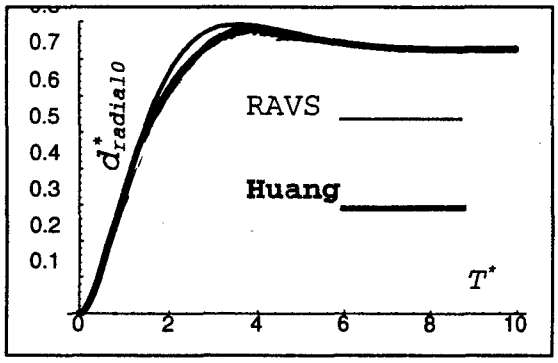

Figure 20. Nondimensional displacement, 0-th mode, $q=0$, $M=9.09184$.

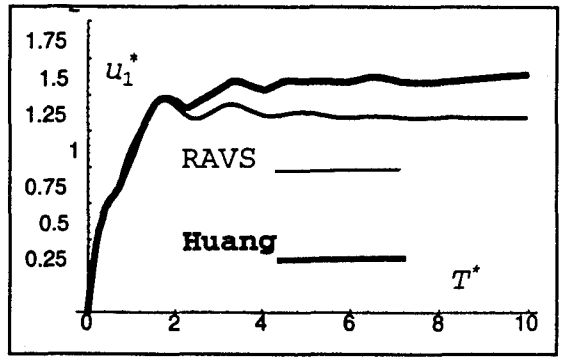

Figure 21. Nondimensional velocity vs. time, 1-st mode, $q=0$, $M=9.09184$.

Situation with $M=4.4189$, $h/a_1=1/69$, $C^2=12.581197$, and $q=4.8c/a_1$

The velocities for the situation with $M=4.4189$, $h/a_1=1/69$, $C^2=12.581197$, and $q=4.8c/a_1$ were calculated for various locations and presented in Figures 22-26. These figures show that the RAVS calculations agree very well with the exact calculations for all locations and times.

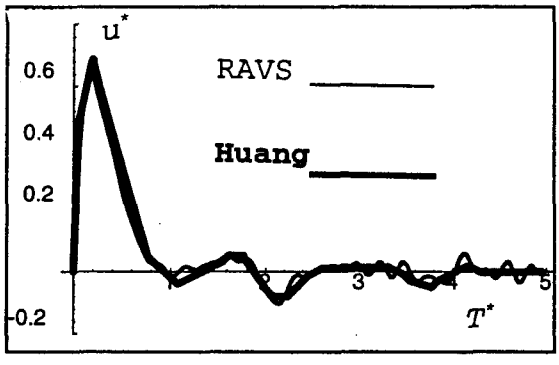

Figure 22. Nondimensional velocity vs. time, $\theta=0$, $q=4.8c/a_1$, $M=4.4189$.

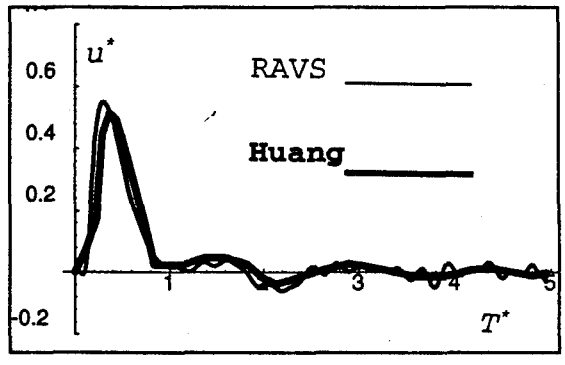

Figure 23. Nondimensional velocity vs. time, $\theta=\pi/6$, $q=4.8c/a_1$, $M=4.4189$.

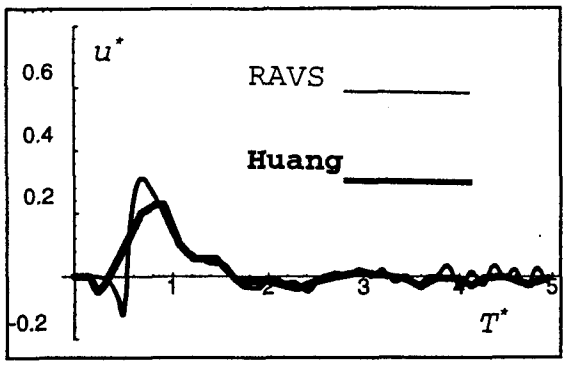

Figure 24. Nondimensional velocity vs. time, $\theta=\pi/3$, $q=4.8c/a_1$, $M=4.4189$.

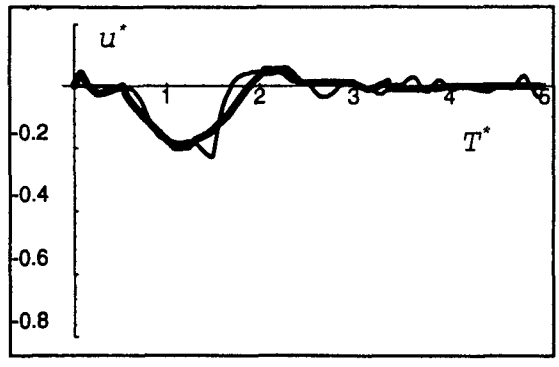

Figure 25. Nondimensional velocity vs. time, $\theta=2\pi/3$, $q=4.8c/a_1$, $M=4.4189$.

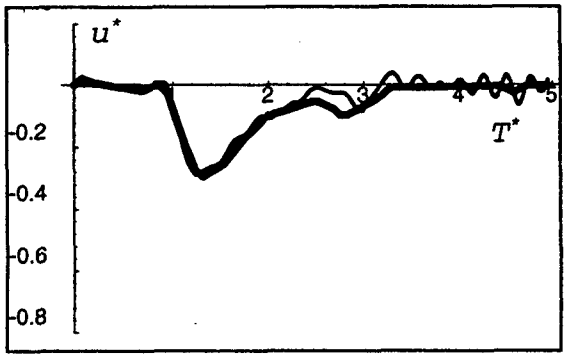

Figure 26. Nondimensional velocity vs. time, $\theta=\pi$, $q=4.8c/a_1$, $M=4.4189$.

Note that the RAVS calculation for this situation had 24 space intervals from $\theta=0$ to $\theta=\pi$ for the finite-difference calculation as programmed in Appendix C.

RIGID CYLINDERS

It is shown in Ref. 1 that the RAVS calculations for *rigid (and immovable)* cylinders attacked by plane waves are in good agreement with the exact calculations. However, the preceding calculations for elastic cylinders attacked by planar waves are in even better agreement with the exact calculations. Also, in

Ref. 1, RAVS calculations (dashed lines) are compared to Huang's[7] exact calculations (**solid** lines) for a *spherical* wave from a source that is *0.5* from the nearest point on the cylinder (see (2) with $p_{hydro}=p_{rad}=0$, $a_1=1$, and $c=1$) and has a step pressure $p(t)=0.5/r$, for $0 \le t$, see Figure 27. It is seen that the error for 0 degrees is very small. The exact pressures at 90, 120, and 180 degrees are so much smaller than that at 0 degrees, that for many purposes they can be disregarded (at these angles, the RAVS calculations give zero pressure). Similar remarks apply to Figure 28. Because the RAVS calculations for the elastic case are in better agreement with the exact calculations for planar waves, it is plausible that the agreement for the elastic case would be in better agreement for spherical waves. Thus, it is plausible that the RAVS calculations for spherical waves would be almost the same as the exact calculations. This is important because spherical waves are of much more practical interest than planar waves.

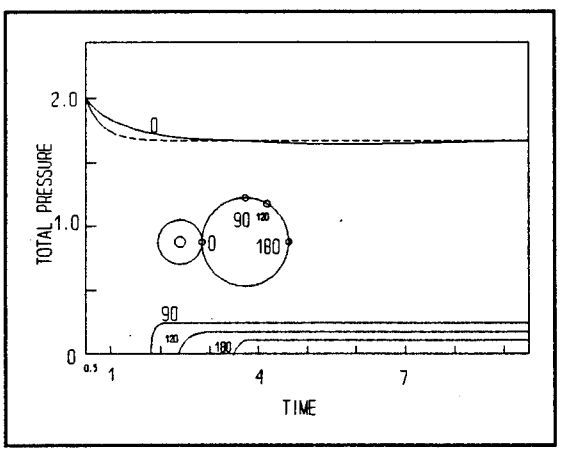

Figure 27. Rigid cylinder attacked by a spherical wave with constant pressure, nearest distance = $0.5a_1$, longitudinal distance = 0.

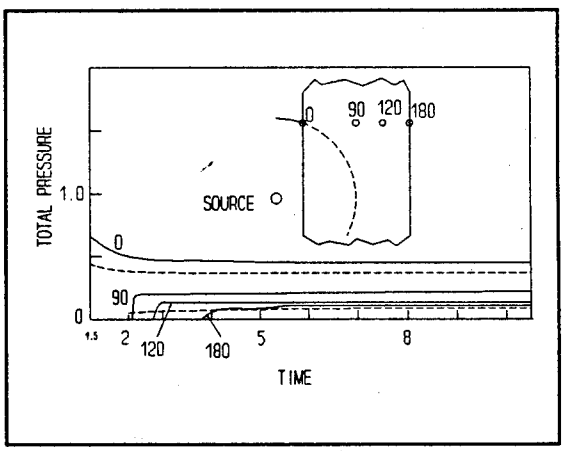

Figure 28. Rigid cylinder attacked by a spherical wave with constant pressure, nearest distance = $0.5a_1$, longitudinal distance = $1.41421a_1$.

SUMMARY AND CONCLUSIONS

An equation of motion (1) for a structural surface was presented. The equations for the pressure that develops when an acoustic wave interacts with a curved and compliant surface were presented ((2)-(14)). These equations were derived using the RAVS model.[1,2] With these equations, an expression for the velocity ((15)-(20)) of the structural surface was derived from the equation of motion, and a numerical method was presented for using this expression. This was applied to the case of a planar wave attacking an elastic cylindrical shell. Hence, a computer program was written for this problem. Calculations from this program (using the RAVS model) were shown to be in good agreement with all of the exact calculations presented by Huang[4] for all locations and times. Thus, the RAVS model gives a good approximation for an elastic cylinder being attacked by a planar wave.

It was shown that the RAVS approximation is even better for spherical attacking waves which are of much more practical interest. In these situations, the *source* of the attacking wave is a *finite* distance from the structural surface. In the limit of the source being very close to a structural surface, the structural surface can be considered as planar. In this situation, the RAVS approximation becomes exact for both a rigid surface and a free surface.

Of course, the results of the RAVS model should be compared to other exact calculations such as those for an elastic spherical shell.[8]

THIS PAGE IS INTENTIONALLY BLANK.

APPENDIX A

SOLUTION OF THE EQUATION OF MOTION

Substituting (14) (for p_{rad}) in (2) (for p_{tot}) and the resulting expression in the equation of motion (1) gives

$$m\dot{u}(t) = p_{hydro} + p(t) + p_{scat}(t) - e^{-\frac{ct}{b}} \int_{-r/c}^{t} e^{\frac{ct'}{b}} \frac{\rho c \dot{u}(t')}{\cos\beta} dt' - p_{str}(t) . \quad (63)$$

Although, $cos\beta$ in (63) must be positive, it might be small and cause difficulties (such as numerical instabilities) in numerical calculations because it appears with the *unknown* velocity on the *right-hand side* of this equation. To avoid these difficulties, the equation of motion for the structural surface is expressed in an equivalent form that is well-behaved even when $cos\beta$ is small. To do this, (63) is transformed so that $u(t)$ does not appear on the right-hand side of the equation. The contribution of the pressure of the scattered wave in this equation is then expressed as a function of the attacking pressure.

TRANSFORMED EQUATION OF MOTION

Equation (63) can be written as

$$e^{\frac{ct}{b}} \dot{u}(t) = e^{\frac{ct}{b}} \frac{p_q(t)}{m} - \int_{-r/c}^{t} e^{\frac{ct'}{b}} \frac{\rho c \dot{u}(t')}{m\cos\beta} dt' , \quad (64)$$

where

$$p_q(t) = p(t) + p_{scat}(t) - [p_{str}(t) - p_{hydro}] . \quad (65)$$

Note that the bracketed term in this equation is zero until the attacking wave arrives at the structure. Differentiating both

sides of (64) gives

$$\frac{d}{dt}\left[e^{\frac{ct}{b}}\dot{u}(t)\right] + \frac{\rho c}{m\cos\beta}\left[e^{\frac{ct}{b}}\dot{u}(t)\right] = \frac{d}{dt}\left[e^{\frac{ct}{b}}\frac{p_q(t)}{m}\right] . \tag{66}$$

Solving this equation gives

$$\begin{aligned} e^{\frac{ct}{b}}\dot{u}(t) &= e^{-\frac{\rho c}{m\cos\beta}t}\int_{-r/c}^{t} e^{\frac{\rho c}{m\cos\beta}t'}\frac{d}{dt'}\left[e^{\frac{ct'}{b}}\frac{p_q(t')}{m}\right]dt' \\ &= e^{\frac{ct}{b}}\frac{p_q(t)}{m} - \frac{\rho c}{m\cos\beta}e^{-\frac{\rho c}{m\cos\beta}t}\int_{-r/c}^{t} e^{\left(\frac{c}{b}+\frac{\rho c}{m\cos\beta}\right)t'}\frac{p_q(t')}{m}dt' . \end{aligned} \tag{67}$$

Thus, we obtain a transformed equation of motion,

$$\begin{aligned} m\dot{u}(t) &= p_q(t) - \left(\eta - \frac{c}{b}\right)e^{-\eta t}\int_{-r/c}^{t} e^{\eta t'}p_q(t')\,dt' \\ &= \dot{I}_q(t) + \frac{c}{b}I_q(t) , \end{aligned} \tag{68}$$

where (see (65))

$$I_q(t) = e^{-\eta t}\int_{-r/c}^{t} e^{\eta t'}p_q(t')\,dt' = I(t) + I_{scat}(t) - I_{str}(t) , \tag{69}$$

in which

$$I(t) = e^{-\eta t}\int_{0}^{t} e^{\eta t'}p(t')\,dt' , \tag{70}$$

$$I_{scat}(t) = e^{-\eta t}\int_{0}^{t} e^{\eta t'}p_{scat}(t')\,dt' , \tag{71}$$

$$I_{str}(t) = e^{-\eta t}\int_{-r/c}^{t} e^{\eta t'}[p_{str}(t') - p_{hydro}]\,dt', \tag{72}$$

and

$$\eta = \frac{c}{b} + \frac{\rho c}{m\cos\beta} , \tag{73}$$

is called "the damping coefficient."* The lower limit of the integration in (70) and (71) is zero because the pressure of the attacking wave and, thus, the pressure of the scattered wave are zero before their arrival at $t=0$. Therefore, the transformed equation of motion (68) can be written as

$$m\dot{u}(t) = \dot{I}(t) + \frac{c}{b}I(t) + \dot{I}_{scat}(t) + \frac{c}{b}I_{scat}(t) - \dot{I}_{str}(t) - \frac{c}{b}I_{str}(t) . \tag{74}$$

SCATTERED PRESSURE CONTRIBUTION AS A FUNCTION OF ATTACKING PRESSURE

From (4), it is seen that

$$\dot{p}_{scat}(t) + \frac{c}{b}p_{scat}(t) = \left[\dot{p}(t) + \frac{c}{r}p(t)\right]\frac{\cos\theta}{\cos\beta} . \tag{75}$$

By performing the integration,

$$e^{-\eta t}\int_0^t e^{-\eta t'}(\qquad)\,dt' , \tag{76}$$

on all of the terms in (75), it is seen that

---

*It can be seen from (69) that

$$\dot{I}_q(t) + \eta I_q(t) = p_q(t) ,$$

which shows that η behaves as a damping coefficient.

$$e^{-\eta t}\int_0^t e^{\eta t'}\dot{p}_{scat}(t')\,dt' + e^{-\eta t}\int_0^t e^{\eta t'}\frac{c}{b}p_{scat}(t')\,dt'$$

$$= \left[e^{-\eta t}\int_0^t e^{\eta t'}\dot{p}(t')\,dt' + e^{-\eta t}\int_0^t e^{\eta t'}\frac{c}{r}p(t')\,dt'\right]\frac{\cos\theta}{\cos\beta}\,. \qquad (77)$$

By integrating by parts, it is seen that

$$e^{-\eta t}\int_0^t e^{\eta t'}\dot{p}_{scat}(t')\,dt'$$

$$= p_{scat}(t) - \eta e^{-\eta t}\int_0^t e^{\eta t'}p_{scat}(t')\,dt' \qquad (78)$$

$$= \frac{d}{dt}\left[e^{-\eta t}\int_0^t e^{\eta t'}p_{scat}(t')\,dt'\right].$$

This * demonstrates that the operation of (76) on the derivative of a function equals the derivative of the operation (76) on that function. Thus, (77) is the same as

$$\frac{d}{dt}\left[e^{-\eta t}\int_0^t e^{\eta t'}p_{scat}(t')\,dt'\right] + \frac{c}{b}e^{-\eta t}\int_0^t e^{\eta t'}p_{scat}(t')\,dt'$$

$$= \left\{\frac{d}{dt}\left[e^{-\eta t}\int_0^t e^{\eta t'}p(t')\,dt'\right] + \frac{c}{r}e^{-\eta t}\int_0^t e^{\eta t'}p(t')\,dt'\right\}\frac{\cos\theta}{\cos\beta}\,. \qquad (79)$$

By substituting (70) and (71), this becomes

---

*The pressure of the incident wave and, thus, the pressure of the scattered wave are zero in the limit of positive time going to zero. If there is a sudden rise in the pressure at time zero, the pressure can be represented (to any desired accuracy) by a function that is zero in the limit of positive time going to zero. The function would then increase at an arbitrarily high rate of change up to its first peak pressure.

$$\dot{I}_{scat}(t) + \frac{c}{b} I_{scat}(t) = \left[\dot{I}(t) + \frac{c}{r} I(t)\right] \frac{\cos\theta}{\cos\beta} \ . \qquad (80)$$

EQUIVALENT EQUATION OF MOTION

Substituting (80) in (74) gives an equivalent equation of motion,

$$m\dot{u}(t) = \dot{I}(t) + \frac{c}{b} I(t) + \left[\dot{I}(t) + \frac{c}{r} I(t)\right] \frac{\cos\theta}{\cos\beta} - \dot{I}_{str}(t) - \frac{c}{b} I_{str}(t) , \qquad (81)$$

where $I(t)$ and $I_{str}(t)$ are determined by (70) and (72). The right-hand side of (81) does not involve the (unknown) velocity (as in (63)). However, the right-hand side does require the mass density of the structural surface and the structural resistance pressure. Integration of both sides of (81) and dividing both sides of the resulting expression by m gives the velocity of the structural surface,

$$u(t) = \frac{I(t)}{m}\left(1 + \frac{\cos\theta}{\cos\beta}\right) + \frac{1}{m}\left(\frac{c}{b} + \frac{c}{r}\frac{\cos\theta}{\cos\beta}\right)\left[\frac{1}{\eta}\int_0^t p(t')\,dt' - \frac{I(t)}{\eta}\right]$$

$$- \frac{I_{str}(t)}{m} - \frac{c}{mb}\left\{\frac{1}{\eta}\int_{-r/c}^{t} [p_{str}(t') - p_{hydro}]\,dt' - \frac{I_{str}(t)}{\eta}\right\} , \qquad (82)$$

see (15)-(20) of the main text.

THIS PAGE IS INTENTIONALLY BLANK.

APPENDIX B

STRUCTURAL RESISTANCE PRESSURE

In this appendix, the notation in Huang's paper[4] is used for the expressions in the first section. In the second section, these expressions are converted to the notation of the main text to obtain the structural resistance pressure.

HUANG'S NOTATION

Equations (8) and (9) of Huang's paper[4] state that

$$\frac{d^2 w_n}{dT^2} + A_n w_n + B_n v_n = -MP_n(1,T)$$

$$\frac{d^2 v_n}{dT^2} + C_n v_n + D_n w_n = 0$$

$$n = 0,1,2,\ldots$$

where

$$A_n = C^2[1 + n^4 h^2/(3a^2)]$$

$$B_n = D_n = nC^2[1 + n^2 h^2/(3a^2)]$$

$$C_n = n^2 C^2[1 + h^2/(3a^2)] \ , \qquad (83)$$

where Eq. (5) of Huang's paper states that

$$P(1,\theta,T) = \sum_{n=0}^{\infty} P_n(1,T)\cos(n\theta) \ ,$$

$$w(\theta,T) = \sum_{n=0}^{\infty} w_n(T)\cos(n\theta) \ ,$$

$$v(\theta,T) = \sum_{n=1}^{\infty} v_n(T)\sin(n\theta) \ , \qquad (84)$$

and Eq. (1) of Huang's paper states that

$$T = ct/a\ ,\quad w = \delta_r/a\ ,\quad v = \delta_\theta/a,\quad P(1,\theta,T) = p(a,\theta,t)/(\rho c^2)\ ,$$

$$M = \rho a/(2h\rho_s)\ ,\quad C^2 = E/[\rho_s(1-\nu^2)c^2]\ , \tag{85}$$

where

c = *acoustic wave speed,*

t = *time after arrival of the wave front at the shell,*

a = *middle surface radius of the cylindrical shell,*

δ_r = *radial deflection ,*

δ_θ = *circumferential deflection,*

$p(a,\theta,t)$ = *total pressure in the fluid at the shell,*

ρ = *unperturbed mass density of the fluid,*

h = *half thickness of the shell,*

ρ_s = *mass density of the shell material,*

E = *Young's modulus of the shell material, and*

ν = *Poisson's ratio of shell material.*

(86)

Performing the operation,

$$\sum_{n=0}^{\infty} \cos(n\theta)\ , \tag{87}$$

on both sides of the first equation in (83) and using (84) yields

$$\frac{\partial^2 w}{\partial T^2} + C^2 w + \frac{C^2h^2}{3a^2}w^{(4)} + C^2 v^{(1)} - \frac{C^2h^2}{3a^2}v^{(3)} = -MP(1,\theta,T)\ , \tag{88}$$

where the superscripts (in parentheses) indicate partial differentiation with respect to θ. Also, performing the operation,

$$\sum_{n=1}^{\infty} \sin(n\theta) \ , \tag{89}$$

on both sides of the second equation in (83) yields

$$\frac{\partial^2 v}{\partial T^2} - C^2\left(1 + \frac{h^2}{3a^2}\right)v^{(2)} - C^2 w^{(1)} + \frac{C^2 h^2}{3a^2} w^{(3)} = 0 \ . \tag{90}$$

Substituting (85), in (88) and (90) and multiplying the resulting equations by

$$\frac{2h\rho_s}{a/c^2} \tag{91}$$

gives

$$2h\rho_s \frac{\partial^2 \delta_r}{\partial t^2} + \frac{2Eh}{(1-\nu^2)a^2}\left[\delta_r + \frac{h^2}{3a^2}\delta_r^{(4)} + \delta_\theta^{(1)} - \frac{h^2}{3a^2}\delta_\theta^{(3)}\right] = -p \tag{92}$$

and

$$2h\rho_s \frac{\partial^2 \delta_\theta}{\partial t^2} + \frac{2Eh}{(1-\nu^2)a^2}\left[-\left(1 + \frac{h^2}{3a^2}\right)\delta_\theta^{(2)} - \delta_r^{(1)} + \frac{h^2}{3a^2}\delta_r^{(3)}\right] = 0 \ . \tag{93}$$

CONVERSION TO NOTATION IN MAIN TEXT

The following variables in the main text [see (1), for m and p_{tot}; see (48), for d_{radial} and d_θ; and see (7) for a_1], are now defined using Huang's notation:

$$\begin{aligned} m &= 2h\rho_s \ , \ Huang, \\ d_{radial} &= -\delta_r \ , \ Huang, \\ d_\theta &= \delta_\theta \ , \ Huang \\ a_1 &= a \ , \ Huang, \\ p_{tot} &= p \ , \ Huang. \end{aligned} \tag{94}$$

Thus, (92) becomes

$$-m\frac{\partial^2 d_{radial}}{\partial t^2} + \frac{2Eh}{(1-\nu^2)\,a_1^{\,2}}\left[-d_{radial} - \frac{h^2}{3a_1^{\,2}}d_{radial}^{(4)} + d_\theta^{(1)} - \frac{h^2}{3a_1^{\,2}}d_\theta^{(3)}\right] = -p_{tot} \tag{95}$$

or

$$m\frac{\partial^2 d_{radial}}{\partial t^2} = p_{tot} - p_{str}\ , \tag{96}$$

where (see the equation of motion (1))

$$p_{str} = \frac{2Eh}{(1-\nu^2)\,a_1^{\,2}}\left[d_{radial} + \frac{h^2}{3a_1^{\,2}}d_{radial}^{(4)} - d_\theta^{(1)} + \frac{h^2}{3a_1^{\,2}}d_\theta^{(3)}\right], \tag{97}$$

is the structural resistance pressure, see (48) in the main text. Also, (93) becomes

$$m\frac{\partial^2 d_\theta}{\partial t^2} + \frac{2Eh}{(1-\nu^2)\,a_1^{\,2}}\left[-\left(1 + \frac{h^2}{3a_1^{\,2}}\right)d_\theta^{(2)} + d_{radial}^{(1)} - \frac{h^2}{3a_1^{\,2}}d_{radial}^{(3)}\right] = 0\ , \tag{98}$$

see (49) in the main text.

APPENDIX C

COMPUTER PROGRAM

The following finite-difference program is written in the *Mathematica*[5] language. Because the variable names are similar to those in the text, it should be fairly easy to follow and modify. A sample run is also included.

```
Date[]
Print[""];
Print["          THE VIRTUAL-SOURCE MODEL          "];
Print[""];
Print["      APPLIED TO AN ELASTIC CYLINDER        "];
Print[""];
Print["          FOR A PLANAR SHOCK WAVE           "];
Print[""];

(* See Huang, Eq. 1 and his discussion before Eq. 25. *)
(*    MHuang=rho*a1/(2*h*rhos);
      CHuang2=E/(rhos*(1-nu^2)*c^2)) *)
(* MHuang=2;       ha=1/31;  CHuang2=13.685665; *)
 MHuang=4.41890; ha=1/69;  CHuang2=12.581197;
(*  MHuang=6.41975; ha=1/100; CHuang2=13.685665;*)
(*  MHuang=9.09184; ha=1/142; CHuang2=12.581197;*)
a1=1.; rho=1.; c=1.; (* Non-dimensional results are the
                        same for all positive values of
                        a1, rho, and c.  *)
q=0; (* q=c/a1; 3*c/a1; 4.8*c/a1;
        q is the same as beta*c/a1 in Huang, Eq. 25.  *)

Omega=1.; (* Non-dimensional results are the same for all
             non-zero values of Omega.  *)
p0=Omega; (* See Huang, Eq. 25. *)
mass=rho*a1/MHuang; kH=(rho*c*c/a1)*CHuang2/MHuang;
rhocmass=rho*c/mass;
h2=ha*ha/3;

nmax=12; (* = maximum number of space intervals
                from 0 to Pi *)
Dtheta=N[Pi]/nmax;
mmax=750; (* = maximum number of time intervals
                from 0 to ttmax *)
ttmax=2.5*a1/c;
Dtime=ttmax/mmax;
mPrint=15; (* = interval between printing *)
```

```
DyDx[y_,Deltax_,sgn_]:=Module[{dummy},
   (* sgn=1, y even;  sgn=-1, y odd *)
   ya=Drop[Join[sgn*Take[y,{2,2}],y],-1];
   Lm1=Length[y]-1;
   yb=Drop[Join[y,sgn*Take[y,{Lm1,Lm1}]],1];
   (yb-ya)/(2*Deltax) (* = rate of change of y *)]

Sh[x_]:=If[x==0, 1, Sinh[x]/x ]

etaF[theta_]:=Module[{dummy},
   S2=(Sin[theta/2])^2; SS=Sqrt[1+8.*S2];
   b=a1*SS; cbeta=(1+2*S2)/SS;
   N[(c/b)+(rho*c/(mass*cbeta))]]



cbF[theta_]:=Module[{dummy},
   S2=(Sin[theta/2])^2; SS=Sqrt[1+8.*S2];
   b=a1*SS;
   N[c/b]]

edF[theta_]:=Module[{dummy},
   eta=etaF[theta];
   2*Exp[-eta*Dtime/2]*Sinh[eta*Dtime/2]/eta]

J0F[t_]:=Module[{dummy},
            If[chi^2 > (epsilon*s)^2,
               eq=Exp[-q*t/2]*Sh[q*t/2];
               ee=Exp[-eta*t/2]Sh[eta*t/2];
               J0=p0*(eq-ee)*t/(eta-q), J0=p0*t*t/2]]

u0F[theta_,tt_]:=Module[{dummy},
   S2=(Sin[theta/2])^2; rMr0=2*a1*S2; t=tt-rMr0/c;
   If[t < 0, 0,
   SS=Sqrt[1+8*S2]; b=a1*SS; cbeta=(1+2*S2)/SS;
   eta=(c/b)+(rho*c/(mass*cbeta));
   s=(eta+q)/2; chi=(eta-q)/2;
   I0=p0*t*Exp[-s*t]*Sh[chi*t];
   epsilon=0.0001;
   If[q*t > epsilon,
      If[eta*t > epsilon,
         cs=Cosh[chi*t]+s*t*Sh[chi*t];
         J0=p0*(1-Exp[-s*t]*cs)/(q*eta),J0F[t]],J0F[t]];
   ctheta=Cos[theta];
   u0m=I0*(1+ctheta/cbeta)+(c/b)*J0;
   u0m/mass ] ]

etaT=Table[etaF[n*Dtheta],{n,0,nmax}];
edT=Table[edF[n*Dtheta],{n,0,nmax}];
cbT=Table[cbF[n*Dtheta],{n,0,nmax}];
u=Table[0,{n,0,nmax}]; ustr=u; Istr=u; dr=u; v=u; dth=u;
urc0=strainrc20=
      Table[0.,{n,0,nmax},{m,0,Floor[mmax/mPrint]}];
dr0rc20a=u1rc0=Table[0.,{m,0,Floor[mmax/mPrint]}];
Do[tt=N[m*Dtime];
```

```
    u0=Table[u0F[n*Dtheta,tt],{n,0,nmax}];
    dr1=DyDx[dr,Dtheta,1]; dr2=DyDx[dr1,Dtheta,-1];
    dr3=DyDx[dr2,Dtheta,1];dr4=DyDx[dr3,Dtheta,-1];
    dth1=DyDx[dth,Dtheta,-1]; dth2=DyDx[dth1,Dtheta,1];
    dth3=DyDx[dth2,Dtheta,-1];
    pstr=kH*(dr+h2*dr4-dth1+h2*dth3); strain=(dth1-dr)/a1;
    DIstr=(pstr-etaT*Istr)*edT; Istr=Istr+DIstr;
    Dustr=(DIstr+Istr*cbT*Dtime)/mass;
    ustr=ustr+Dustr; uL=u; u=u0-ustr;
    If[IntegerQ[m/mPrint], mP=m/mPrint;
          Print[" "]; Print["c*tt/a1 = ",c*tt/a1];
          Print["u*rho*c/Omega = ",Chop[u*rho*c/Omega]];
          Print["strain*rho*c^2/Omega = ",
                 Chop[strain*rho*c^2/Omega]];
          dr0=(.5*(dr[[1]]+dr[[nmax+1]])
               +Sum[dr[[n]],{n,2,nmax}])/nmax;
          u1=(.5*(u[[1]]-u[[nmax+1]])
               +Sum[u[[n]]*Cos[(n-1)*N[Pi]/nmax]
               ,{n,2,nmax}])*2/nmax;
          Print[
             "dr0*rho*c^2/(Omega*a1) = ",
              dr0*rho*c^2/(Omega*a1),
             "  u1*rho*c/Omega= ",u1*rho*c/Omega];
          Do[      urc0[[n+1,mP+1]]
                      =u[[n+1]]*rho*c/Omega;
             strainrc20[[n+1,mP+1]]
                 =strain[[n+1]]*rho*c^2/Omega;
             ,{n,0,nmax}];
          dr0rc20a[[mP+1]]=dr0*rho*c^2/(Omega*a1);
          u1rc0[[mP+1]]=u1*rho*c/Omega;
       ,dumb=0];
    dr=dr+(u+uL)*Dtime/2;
    vd=(kH/mass)*((1+h2)*dth2-dr1+h2*dr3);
    vL=v; v=v+vd*Dtime; dth=dth+(v+vL)*Dtime/2;
, {m,0,mmax}];
urc0 >> urc0.dat;
strainrc20 >> strc20.dat;
dr0rc20a >> drc20a.dat;
u1rc0 >> u1rc0.dat;
Print["DONE"]
```

```
{1996, 1, 30, 16, 59, 28}

         THE VIRTUAL-SOURCE MODEL

      APPLIED TO AN ELASTIC CYLINDER

         FOR A PLANAR SHOCK WAVE


c*tt/a1 = 0
u*rho*c/Omega = {0, 0, 0, 0, 0, 0, 0, 0, 0, 0, 0, 0, 0}
strain*rho*c^2/Omega = {0, 0, 0, 0, 0, 0, 0, 0, 0, 0, 0, 0, 0}
dr0*rho*c^2/(Omega*a1) = 0  u1*rho*c/Omega= 0
```

```
c*tt/a1 = 0.05
                                                    -6            -7
u*rho*c/Omega = {0.390278, 0.134938, -1.754 10   , 1.31981 10   ,
                -6            -8
   -1.73709 10   , -4.87924 10   , 0, 0, 0, 0, 0, 0, 0}
strain*rho*c^2/Omega = {-0.00878012, -0.000692333, -0.0000658705,
              -7             -7             -10             -10
   -2.6909 10   , -1.34421 10   , 1.11087 10    , -1.11216 10    , 0, 0, 0,
   0, 0, 0}
dr0*rho*c^2/(Omega*a1) = 0.000429056  u1*rho*c/Omega= 0.0542462

c*tt/a1 = 0.1
u*rho*c/Omega = {0.68735, 0.491574, -0.00024465, -0.0000248791,
                           -6             -8             -10
   -0.000015459, -4.00469 10   , -1.20485 10   , -1.84257 10    , 0, 0, 0,
   0, 0}
strain*rho*c^2/Omega = {-0.0327916, -0.0153423, -0.00119008,
                                              -7             -8
   -0.000216349, -0.0000148417, -9.67291 10   , -9.06537 10   ,
                -9             -10
   -2.01236 10   , -3.1317 10    , 0, 0, 0, 0}
dr0*rho*c^2/(Omega*a1) = 0.00276337  u1*rho*c/Omega= 0.136377

c*tt/a1 = 0.15
u*rho*c/Omega = {0.906989, 0.758442, 0.130266, -0.000555736, -0.00008591,
                             -7             -8             -9
   -0.0000269907, -6.22903 10   , -5.07746 10   , -3.78493 10   , 0, 0, 0, 0}
strain*rho*c^2/Omega = {-0.0627982, -0.0440431, -0.00636443, -0.00216181,
                                                 -6             -7
   -0.000180932, -0.0000378213, -2.85768 10   , -3.28619 10   ,
                -8             -9             -10
   -2.63074 10   , -1.64085 10   , -1.55108 10    , 0, 0}
dr0*rho*c^2/(Omega*a1) = 0.00701587  u1*rho*c/Omega= 0.216411

c*tt/a1 = 0.2
u*rho*c/Omega = {1.06626, 0.950778, 0.469704, -0.00322633, -0.000435931,
                                       -6             -7             -8
   -0.000146382, -0.000011791, -1.47 10   , -1.13404 10   , -1.31009 10   ,
                -9
   -1.1139 10   , 0, 0}
strain*rho*c^2/Omega = {-0.0900519, -0.0796894, -0.0304906, -0.00849706,
                                                           -6
   -0.00117721, -0.000334082, -0.0000303624, -6.61006 10   ,
                -7             -8             -9             -10
   -5.26616 10   , -7.67038 10   , -6.06395 10   , -5.77085 10    , 0}
dr0*rho*c^2/(Omega*a1) = 0.013771  u1*rho*c/Omega= 0.309292

c*tt/a1 = 0.25
u*rho*c/Omega = {1.18173, 1.08383, 0.713623, -0.0108063, -0.00207721,
                                                        -6
   -0.000665031, -0.0000820345, -0.0000158027, -1.40114 10   ,
                -7             -8             -9             -10
   -2.7135 10   , -2.21772 10   , -3.20792 10   , -5.12757 10    }
strain*rho*c^2/Omega = {-0.110981, -0.115601, -0.0727123, -0.021653,
                                                                 -6
   -0.00536965, -0.00153255, -0.00020353, -0.0000547712, -5.25935 10   ,
                -6             -8             -8             -9
   -1.15562 10   , -9.65689 10   , -1.60209 10   , -2.54973 10   }
dr0*rho*c^2/(Omega*a1) = 0.0227186  u1*rho*c/Omega= 0.374488

c*tt/a1 = 0.3
u*rho*c/Omega = {1.26616, 1.17245, 0.877804, 0.029222, -0.00758226,
                                                              -6
   -0.00234143, -0.000401832, -0.0000971238, -0.0000110074, -2.6893 10   ,
                -7             -8             -9
   -2.49546 10   , -5.09881 10   , -8.47793 10   }
strain*rho*c^2/Omega = {-0.128169, -0.146546, -0.122157, -0.0426228,
   -0.016362, -0.00480748, -0.00096836, -0.000274106, -0.0000354739,
                -6             -7             -7             -8
```

```
   -9.23502 10   , -9.20385 10   , -2.06215 10   , -3.53533 10   }
dr0*rho*c^2/(Omega*a1) = 0.0331557  u1*rho*c/Omega= 0.42368

c*tt/a1 = 0.35
u*rho*c/Omega = {1.32684, 1.23031, 0.980321, 0.338326, -0.020849,
   -0.00655868, -0.00154461, -0.000417103, -0.000062901, -0.0000169489,
              -6             -7             -8
   -1.93476 10   , -4.75978 10   , -8.93905 10   }
strain*rho*c^2/Omega = {-0.147291, -0.169524, -0.167398, -0.0802541,
   -0.0370165, -0.0118034, -0.00337508, -0.000985651, -0.000176098,
                           -6             -6             -7
   -0.0000489309, -6.22838 10   , -1.62146 10   , -3.24261 10   }
dr0*rho*c^2/(Omega*a1) = 0.0453529  u1*rho*c/Omega= 0.48801

c*tt/a1 = 0.4
u*rho*c/Omega = {1.36622, 1.26871, 1.04042, 0.549674, -0.0458149,
   -0.0155475, -0.00475985, -0.001385, -0.000275576, -0.0000779002,
                           -6             -7
   -0.0000112943, -3.06547 10   , -6.83805 10   }
strain*rho*c^2/Omega = {-0.173062, -0.184802, -0.200042, -0.133486,
   -0.0676164, -0.0250382, -0.00914231, -0.00281387, -0.000671982,
                                       -6             -6
   -0.000193887, -0.0000320787, -9.02277 10   , -2.1991 10   }
dr0*rho*c^2/(Omega*a1) = 0.0591983  u1*rho*c/Omega= 0.528656

c*tt/a1 = 0.45
u*rho*c/Omega = {1.38455, 1.29527, 1.07588, 0.681945, -0.0847244,
   -0.0326425, -0.0121164, -0.00380232, -0.000964665, -0.000283381,
                                       -6
   -0.0000520526, -0.0000149929, -4.05749 10   }
strain*rho*c^2/Omega = {-0.206103, -0.195723, -0.2172, -0.189263,
   -0.105065, -0.0473296, -0.0203005, -0.00681753, -0.00205813,
   -0.000619582, -0.000131101, -0.0000388247, -0.0000116707}
dr0*rho*c^2/(Omega*a1) = 0.0739668  u1*rho*c/Omega= 0.551379

c*tt/a1 = 0.5
u*rho*c/Omega = {1.38303, 1.31357, 1.10023, 0.756233, -0.136777,
   -0.0616435, -0.0262858, -0.00905239, -0.00279995, -0.000861915,
   -0.000196245, -0.0000592985, -0.0000194509}
strain*rho*c^2/Omega = {-0.24203, -0.206774, -0.221796, -0.23533,
   -0.143549, -0.0798836, -0.0384272, -0.0145521, -0.00525634,
   -0.00168049, -0.000440301, -0.000137011, -0.000050294}
dr0*rho*c^2/(Omega*a1) = 0.0890722  u1*rho*c/Omega= 0.561356

c*tt/a1 = 0.55
u*rho*c/Omega = {1.36612, 1.32405, 1.121, 0.794122, 0.107007, -0.105335,
   -0.0498887, -0.019213, -0.00694996, -0.00227573, -0.00062361,
   -0.000198169, -0.0000776547}
strain*rho*c^2/Omega = {-0.273095, -0.221529, -0.22066, -0.263712,
   -0.183344, -0.120828, -0.063793, -0.0278615, -0.0115378, -0.00400039,
   -0.00125217, -0.000413182, -0.000181248}
dr0*rho*c^2/(Omega*a1) = 0.104631  u1*rho*c/Omega= 0.588568

c*tt/a1 = 0.6
u*rho*c/Omega = {1.34179, 1.32567, 1.13979, 0.814657, 0.270561,
   -0.163875, -0.084728, -0.0369165, -0.0151172, -0.00534854, -0.0017124,
   -0.00057744, -0.000264697}
strain*rho*c^2/Omega = {-0.291559, -0.241203, -0.221837, -0.272703,
   -0.22432, -0.164998, -0.0954124, -0.0483004, -0.0222821, -0.00853444,
   -0.00309035, -0.001096, -0.00055979}
dr0*rho*c^2/(Omega*a1) = 0.12082  u1*rho*c/Omega= 0.605078

c*tt/a1 = 0.65
u*rho*c/Omega = {1.31976, 1.31769, 1.1537, 0.831515, 0.375294, -0.233867,
   -0.131439, -0.0648301, -0.0293742, -0.0113763, -0.00414687,
   -0.00150054, -0.00078646}
strain*rho*c^2/Omega = {-0.293339, -0.264247, -0.23159, -0.266693,
   -0.257485, -0.205179, -0.131377, -0.0763083, -0.0385975, -0.0165318,
   -0.00675127, -0.00260922, -0.00151212}
```

```
dr0*rho*c^2/(Omega*a1) = 0.137066  u1*rho*c/Omega= 0.615307

c*tt/a1 = 0.7
u*rho*c/Omega = {1.30839, 1.30102, 1.15827, 0.851501, 0.441232,
   -0.308667, -0.189149, -0.104791, -0.0518179, -0.0221458, -0.00900568,
   -0.00353419, -0.00207205}
strain*rho*c^2/Omega = {-0.280369, -0.287027, -0.251465, -0.253976,
   -0.277928, -0.234403, -0.168588, -0.110467, -0.060931, -0.0293271,
   -0.0132694, -0.00565358, -0.00363233}
dr0*rho*c^2/(Omega*a1) = 0.15292  u1*rho*c/Omega= 0.622956

c*tt/a1 = 0.75
u*rho*c/Omega = {1.31148, 1.27865, 1.15075, 0.874968, 0.484809,
   -0.330613, -0.25518, -0.15684, -0.0840954, -0.0397728, -0.0177835,
   -0.00763362, -0.00491012}
strain*rho*c^2/Omega = {-0.260442, -0.305222, -0.277531, -0.243406,
   -0.285732, -0.248481, -0.203013, -0.147248, -0.0887421, -0.047942,
   -0.0237822, -0.0112609, -0.0078662}
dr0*rho*c^2/(Omega*a1) = 0.168043  u1*rho*c/Omega= 0.633154

c*tt/a1 = 0.8
u*rho*c/Omega = {1.32667, 1.25515, 1.1324, 0.897965, 0.517252, -0.151369,
   -0.325165, -0.218549, -0.126886, -0.0663104, -0.0323033, -0.0152529,
   -0.0105897}
strain*rho*c^2/Omega = {-0.244415, -0.315389, -0.302186, -0.241256,
   -0.284926, -0.255, -0.230604, -0.181612, -0.120333, -0.0725717,
   -0.0393023, -0.0207696, -0.015532}
dr0*rho*c^2/(Omega*a1) = 0.182827  u1*rho*c/Omega= 0.654286

c*tt/a1 = 0.85
u*rho*c/Omega = {1.34624, 1.23551, 1.10859, 0.915125, 0.544341,
   -0.0171408, -0.393764, -0.285228, -0.179471, -0.10316, -0.0544994,
   -0.0283824, -0.0209926}
strain*rho*c^2/Omega = {-0.241845, -0.316134, -0.317649, -0.249897,
   -0.281069, -0.259464, -0.248512, -0.208936, -0.152945, -0.102151,
   -0.0604353, -0.0356691, -0.028224}
dr0*rho*c^2/(Omega*a1) = 0.197325  u1*rho*c/Omega= 0.677174

c*tt/a1 = 0.9
u*rho*c/Omega = {1.36015, 1.22377, 1.08697, 0.922142, 0.567654,
   0.0837728, -0.455844, -0.351223, -0.239544, -0.150451, -0.0860863,
   -0.0494446, -0.0385668}
strain*rho*c^2/Omega = {-0.256918, -0.308549, -0.319547, -0.267719,
   -0.278596, -0.262913, -0.256067, -0.22669, -0.183197, -0.134286,
   -0.0871144, -0.0572893, -0.047561}
dr0*rho*c^2/(Omega*a1) = 0.211184  u1*rho*c/Omega= 0.703284

c*tt/a1 = 0.95
u*rho*c/Omega = {1.36019, 1.2219, 1.07435, 0.917561, 0.586764, 0.159416,
   -0.507742, -0.411467, -0.303403, -0.206664, -0.128171, -0.0809948,
   -0.0661173}
strain*rho*c^2/Omega = {-0.286447, -0.295866, -0.308943, -0.28983,
   -0.279066, -0.267091, -0.255019, -0.234941, -0.207834, -0.165712,
   -0.118435, -0.0863688, -0.0747836}
dr0*rho*c^2/(Omega*a1) = 0.224143  u1*rho*c/Omega= 0.733475

c*tt/a1 = 1.
u*rho*c/Omega = {1.34356, 1.22935, 1.07396, 0.903457, 0.601409, 0.214984,
   -0.548124, -0.462743, -0.366573, -0.268742, -0.180898, -0.125228,
   -0.10638}
strain*rho*c^2/Omega = {-0.320901, -0.282446, -0.291901, -0.309826,
   -0.281019, -0.273354, -0.2489, -0.23612, -0.224602, -0.193186,
   -0.152668, -0.122611, -0.110265}
dr0*rho*c^2/(Omega*a1) = 0.236018  u1*rho*c/Omega= 0.768066

c*tt/a1 = 1.05
u*rho*c/Omega = {1.31431, 1.24329, 1.08417, 0.884827, 0.612767, 0.253996,
   -0.383049, -0.504367, -0.424746, -0.332719, -0.243241, -0.183366,
   -0.161404}
```

```
strain*rho*c^2/Omega = {-0.348104, -0.272466, -0.276778, -0.32202,
   -0.281378, -0.281809, -0.246109, -0.234177, -0.233007, -0.214507,
   -0.187483, -0.164381, -0.153053}
dr0*rho*c^2/(Omega*a1) = 0.247058  u1*rho*c/Omega= 0.806907

c*tt/a1 = 1.1
u*rho*c/Omega = {1.28199, 1.25959, 1.09936, 0.86796, 0.623299, 0.279507,
   -0.257114, -0.538117, -0.474942, -0.394744, -0.313019, -0.255083,
   -0.231854}
strain*rho*c^2/Omega = {-0.358095, -0.268705, -0.270472, -0.323323,
   -0.277993, -0.291019, -0.252953, -0.23334, -0.235036, -0.229302,
   -0.220371, -0.208705, -0.200613}
dr0*rho*c^2/(Omega*a1) = 0.257548  u1*rho*c/Omega= 0.849457

c*tt/a1 = 1.15
u*rho*c/Omega = {1.25812, 1.27401, 1.11261, 0.858416, 0.635252, 0.294992,
   -0.165601, -0.567473, -0.516657, -0.452171, -0.387183, -0.338151,
   -0.316395}
strain*rho*c^2/Omega = {-0.347121, -0.271834, -0.275379, -0.314141,
   -0.271591, -0.298435, -0.266084, -0.236855, -0.23501, -0.239227,
   -0.249194, -0.251635, -0.248907}
dr0*rho*c^2/(Omega*a1) = 0.267283  u1*rho*c/Omega= 0.894874

c*tt/a1 = 1.2
u*rho*c/Omega = {1.25172, 1.28349, 1.11881, 0.859329, 0.649089, 0.304607,
   -0.102485, -0.596414, -0.552207, -0.504322, -0.46236, -0.428467,
   -0.41138}
strain*rho*c^2/Omega = {-0.319097, -0.280381, -0.288451, -0.298047,
   -0.265585, -0.301381, -0.280374, -0.246084, -0.237979, -0.247464,
   -0.272723, -0.28897, -0.292929}
dr0*rho*c^2/(Omega*a1) = 0.276121  u1*rho*c/Omega= 0.9421

c*tt/a1 = 1.25
u*rho*c/Omega = {1.26599, 1.28687, 1.11694, 0.870586, 0.662871, 0.312767,
   -0.0603516, -0.628159, -0.585945, -0.552615, -0.535529, -0.520552,
   -0.511028}
strain*rho*c^2/Omega = {-0.28396, -0.291352, -0.302743, -0.280408,
   -0.264359, -0.298225, -0.291068, -0.260237, -0.247764, -0.2576,
   -0.290919, -0.317165, -0.327658}
dr0*rho*c^2/(Omega*a1) = 0.283971  u1*rho*c/Omega= 0.989952

c*tt/a1 = 1.3
u*rho*c/Omega = {1.29719, 1.28509, 1.11037, 0.889117, 0.672974, 0.323237,
   -0.0315234, -0.545523, -0.622659, -0.599946, -0.60459, -0.608452,
   -0.608188}
strain*rho*c^2/Omega = {-0.253658, -0.301255, -0.310713, -0.266525,
   -0.270902, -0.289269, -0.295808, -0.278935, -0.26548, -0.272266,
   -0.304797, -0.334182, -0.349266}
dr0*rho*c^2/(Omega*a1) = 0.290966  u1*rho*c/Omega= 1.03208

c*tt/a1 = 1.35
u*rho*c/Omega = {1.33636, 1.28066, 1.1052, 0.910104, 0.675836, 0.338066,
   -0.00979078, -0.471102, -0.665801, -0.649527, -0.668601, -0.686849,
   -0.695628}
strain*rho*c^2/Omega = {-0.237511, -0.307185, -0.307742, -0.259956,
   -0.284993, -0.277206, -0.295624, -0.302616, -0.289123, -0.29223,
   -0.315846, -0.340024, -0.35624}
dr0*rho*c^2/(Omega*a1) = 0.297452  u1*rho*c/Omega= 1.07261

c*tt/a1 = 1.4
u*rho*c/Omega = {1.37284, 1.27681, 1.10727, 0.928633, 0.669898, 0.356684,
   0.00814026, -0.426323, -0.716211, -0.703714, -0.727575, -0.752115,
   -0.76757}
strain*rho*c^2/Omega = {-0.238862, -0.307618, -0.294296, -0.261615,
   -0.302845, -0.266794, -0.2944, -0.325459, -0.31435, -0.316183,
   -0.325269, -0.336785, -0.35004}
dr0*rho*c^2/(Omega*a1) = 0.303339  u1*rho*c/Omega= 1.1115

c*tt/a1 = 1.45
```

```
u*rho*c/Omega = {1.39832, 1.27646, 1.11941, 0.941156, 0.656772, 0.375792,
   0.0222441, -0.402573, -0.771835, -0.762999, -0.781917, -0.803012,
   -0.821062}
strain*rho*c^2/Omega = {-0.254345, -0.302723, -0.275778, -0.269918,
   -0.318511, -0.263211, -0.296988, -0.34254, -0.336127, -0.340741,
   -0.333352, -0.328171, -0.334951}
dr0*rho*c^2/(Omega*a1) = 0.308559  u1*rho*c/Omega= 1.14761

c*tt/a1 = 1.5
u*rho*c/Omega = {1.4095, 1.28138, 1.13991, 0.946273, 0.640975, 0.39034,
   0.0301133, -0.391146, -0.828514, -0.825409, -0.831749, -0.840862,
   -0.85672}
strain*rho*c^2/Omega = {-0.275917, -0.294148, -0.260174, -0.281783,
   -0.326463, -0.270061, -0.306775, -0.351441, -0.350552, -0.361157,
   -0.3393, -0.318591, -0.317046}
dr0*rho*c^2/(Omega*a1) = 0.313077  u1*rho*c/Omega= 1.18005

c*tt/a1 = 1.55
u*rho*c/Omega = {1.40864, 1.29179, 1.16315, 0.944663, 0.628241, 0.395269,
   0.0289221, -0.38481, -0.788058, -0.886642, -0.876467, -0.86909,
   -0.87853}
strain*rho*c^2/Omega = {-0.294637, -0.28444, -0.254591, -0.294001,
   -0.324194, -0.287882, -0.323805, -0.352668, -0.358195, -0.372712,
   -0.341683, -0.312017, -0.302491}
dr0*rho*c^2/(Omega*a1) = 0.317063  u1*rho*c/Omega= 1.20036

c*tt/a1 = 1.6
u*rho*c/Omega = {1.40174, 1.30641, 1.18185, 0.938311, 0.623084, 0.38738,
   0.0175509, -0.37894, -0.75965, -0.941054, -0.914826, -0.892221,
   -0.892666}
strain*rho*c^2/Omega = {-0.304488, -0.276325, -0.262226, -0.3044,
   -0.313616, -0.313733, -0.344517, -0.349007, -0.361765, -0.372357,
   -0.339498, -0.310915, -0.295707}
dr0*rho*c^2/(Omega*a1) = 0.320705  u1*rho*c/Omega= 1.21755

c*tt/a1 = 1.65
u*rho*c/Omega = {1.39539, 1.32281, 1.19004, 0.929464, 0.626716, 0.366643,
   -0.00214865, -0.371813, -0.738576, -0.98329, -0.945661, -0.914601,
   -0.905638}
strain*rho*c^2/Omega = {-0.304613, -0.272078, -0.281121, -0.312371,
   -0.300546, -0.342, -0.363091, -0.344124, -0.362005, -0.360028,
   -0.333183, -0.315593, -0.298069}
dr0*rho*c^2/(Omega*a1) = 0.323957  u1*rho*c/Omega= 1.23126

c*tt/a1 = 1.7
u*rho*c/Omega = {1.39378, 1.33805, 1.18544, 0.919746, 0.636259, 0.336476,
   -0.0253831, -0.363971, -0.721675, -1.01008, -0.968772, -0.939186,
   -0.922405}
strain*rho*c^2/Omega = {-0.299123, -0.273147, -0.305186, -0.318659,
   -0.292407, -0.366134, -0.373636, -0.340982, -0.359927, -0.339067,
   -0.324775, -0.324175, -0.307695}
dr0*rho*c^2/(Omega*a1) = 0.326792  u1*rho*c/Omega= 1.24136

c*tt/a1 = 1.75
u*rho*c/Omega = {1.39698, 1.34924, 1.17012, 0.909771, 0.645721, 0.302882,
   -0.045742, -0.356965, -0.706917, -0.97434, -0.985484, -0.966768,
   -0.945095}
strain*rho*c^2/Omega = {-0.294747, -0.280042, -0.326984, -0.324609,
   -0.295082, -0.380682, -0.372553, -0.340725, -0.356102, -0.316372,
   -0.317322, -0.333261, -0.320385}
dr0*rho*c^2/(Omega*a1) = 0.329275  u1*rho*c/Omega= 1.24238

c*tt/a1 = 1.8
u*rho*c/Omega = {1.40138, 1.35402, 1.14934, 0.899324, 0.648384, 0.272769,
   -0.0573476, -0.352027, -0.692809, -0.928424, -0.998568, -0.995912,
   -0.972791}
strain*rho*c^2/Omega = {-0.297511, -0.292434, -0.340971, -0.331273,
   -0.310255, -0.382895, -0.360115, -0.342532, -0.350412, -0.300277,
   -0.313733, -0.339184, -0.331364}
```

```
dr0*rho*c^2/(Omega*a1) = 0.331543  u1*rho*c/Omega= 1.2403

c*tt/a1 = 1.85
u*rho*c/Omega = {1.40167, 1.35086, 1.12909, 0.887912, 0.63967, 0.252012,
   -0.0569791, -0.349258, -0.677967, -0.886336, -1.0115, -1.0237,
   -1.00239}
strain*rho*c^2/Omega = {-0.309994, -0.309335, -0.345727, -0.338793,
   -0.334421, -0.373414, -0.340557, -0.344396, -0.34239, -0.295352,
   -0.315535, -0.339413, -0.337135}
dr0*rho*c^2/(Omega*a1) = 0.333575  u1*rho*c/Omega= 1.23642

c*tt/a1 = 1.9
u*rho*c/Omega = {1.39347, 1.33917, 1.11347, 0.875391, 0.619249, 0.243912,
   -0.0452886, -0.347538, -0.66111, -0.853966, -1.00971, -1.04696,
   -1.03018}
strain*rho*c^2/Omega = {-0.33034, -0.329272, -0.344227, -0.346306,
   -0.360071, -0.355868, -0.320571, -0.344219, -0.331944, -0.302715,
   -0.322314, -0.333443, -0.336694}
dr0*rho*c^2/(Omega*a1) = 0.335372  u1*rho*c/Omega= 1.22858

c*tt/a1 = 1.95
u*rho*c/Omega = {1.37538, 1.31937, 1.10316, 0.862328, 0.591466, 0.248476,
   -0.0265827, -0.345076, -0.641472, -0.835444, -1.00608, -1.06355,
   -1.05346}
strain*rho*c^2/Omega = {-0.353348, -0.350414, -0.342067, -0.352386,
   -0.378615, -0.335612, -0.306809, -0.340864, -0.320063, -0.319565,
   -0.332113, -0.322972, -0.331711}
dr0*rho*c^2/(Omega*a1) = 0.337001  u1*rho*c/Omega= 1.2189

c*tt/a1 = 2.
u*rho*c/Omega = {1.34955, 1.29282, 1.09554, 0.849943, 0.563842, 0.262694,
   -0.00722563, -0.340284, -0.619411, -0.831483, -1.00837, -1.06822,
   -1.07162}
strain*rho*c^2/Omega = {-0.372987, -0.370667, -0.344565, -0.35578,
   -0.383853, -0.318091, -0.303398, -0.334722, -0.309069, -0.339953,
   -0.340682, -0.311423, -0.325643}
dr0*rho*c^2/(Omega*a1) = 0.33846  u1*rho*c/Omega= 1.20831

c*tt/a1 = 2.05
u*rho*c/Omega = {1.32057, 1.26179, 1.08642, 0.839658, 0.544211, 0.281617,
   0.00670417, -0.332576, -0.596792, -0.838859, -1.01337, -1.06424,
   -1.08449}
strain*rho*c^2/Omega = {-0.385068, -0.387828, -0.35407, -0.356078,
   -0.374536, -0.307382, -0.310499, -0.327564, -0.302054, -0.3567,
   -0.34397, -0.302962, -0.321983}
dr0*rho*c^2/(Omega*a1) = 0.339764  u1*rho*c/Omega= 1.19736

c*tt/a1 = 2.1
u*rho*c/Omega = {1.29346, 1.22929, 1.07247, 0.832466, 0.537661, 0.299819,
   0.0115623, -0.322709, -0.576766, -0.851266, -1.01682, -1.05773,
   -1.09362}
strain*rho*c^2/Omega = {-0.388818, -0.399822, -0.368763, -0.354031,
   -0.354937, -0.305338, -0.324481, -0.321771, -0.301706, -0.363833,
   -0.339955, -0.300707, -0.322574}
dr0*rho*c^2/(Omega*a1) = 0.34092  u1*rho*c/Omega= 1.18682

c*tt/a1 = 2.15
u*rho*c/Omega = {1.27164, 1.19873, 1.05318, 0.828435, 0.544528, 0.312776,
   0.00724153, -0.312515, -0.562883, -0.86128, -1.01509, -1.05316,
   -1.10207}
strain*rho*c^2/Omega = {-0.386698, -0.405053, -0.38347, -0.351335,
   -0.333185, -0.311495, -0.339607, -0.319286, -0.309042, -0.358663,
   -0.329633, -0.305796, -0.326596}
dr0*rho*c^2/(Omega*a1) = 0.341934  u1*rho*c/Omega= 1.17726

c*tt/a1 = 2.2
u*rho*c/Omega = {1.25595, 1.17353, 1.03144, 0.826567, 0.560275, 0.317782,
   -0.00317018, -0.304156, -0.557809, -0.862788, -1.00673, -1.054,
   -1.11105}
```

```
strain*rho*c^2/Omega = {-0.382655, -0.402782, -0.392086, -0.349989,
   -0.318034, -0.323626, -0.35048, -0.320788, -0.32265, -0.342768,
   -0.316789, -0.316972, -0.33094}
dr0*rho*c^2/(Omega*a1) = 0.342814  u1*rho*c/Omega= 1.16913

c*tt/a1 = 2.25
u*rho*c/Omega = {1.24505, 1.15654, 1.01243, 0.825107, 0.577295, 0.314245,
   -0.0149695, -0.299253, -0.562166, -0.853014, -0.993207, -1.06167,
   -1.11948}
strain*rho*c^2/Omega = {-0.379799, -0.393421, -0.390489, -0.351479,
   -0.315428, -0.338627, -0.3542, -0.325452, -0.338867, -0.321513,
   -0.306555, -0.330952, -0.331815}
dr0*rho*c^2/(Omega*a1) = 0.343566  u1*rho*c/Omega= 1.16282

c*tt/a1 = 2.3
u*rho*c/Omega = {1.23691, 1.14948, 1.0014, 0.822211, 0.587891, 0.303426,
   -0.0239363, -0.298267, -0.574011, -0.833457, -0.978441, -1.07512,
   -1.12466}
strain*rho*c^2/Omega = {-0.378691, -0.378619, -0.378549, -0.356112,
   -0.326257, -0.353388, -0.351347, -0.3314, -0.352938, -0.302234,
   -0.303322, -0.343487, -0.326813}
dr0*rho*c^2/(Omega*a1) = 0.3442  u1*rho*c/Omega= 1.1586

c*tt/a1 = 2.35
u*rho*c/Omega = {1.23051, 1.15256, 1.00125, 0.8167, 0.587218, 0.287823,
   -0.0280455, -0.300443, -0.589274, -0.809359, -0.967295, -1.09119,
   -1.12396}
strain*rho*c^2/Omega = {-0.377153, -0.361051, -0.360339, -0.362784,
   -0.346198, -0.365417, -0.34541, -0.336632, -0.360732, -0.291728,
   -0.308857, -0.35077, -0.31648}
dr0*rho*c^2/(Omega*a1) = 0.344728  u1*rho*c/Omega= 1.15661

c*tt/a1 = 2.4
u*rho*c/Omega = {1.2268, 1.16436, 1.0112, 0.808624, 0.574998, 0.270469,
   -0.0280858, -0.304303, -0.603049, -0.787907, -0.963596, -1.10569,
   -1.11656}
strain*rho*c^2/Omega = {-0.371662, -0.34392, -0.342417, -0.36928,
   -0.367632, -0.373117, -0.340987, -0.340004, -0.36033, -0.293922,
   -0.321486, -0.35071, -0.304582}
dr0*rho*c^2/(Omega*a1) = 0.345161  u1*rho*c/Omega= 1.15688

c*tt/a1 = 2.45
u*rho*c/Omega = {1.22837, 1.18202, 1.027, 0.7994, 0.55539, 0.254318,
   -0.0269805, -0.308474, -0.611293, -0.775767, -0.968538, -1.11482,
   -1.10462}
strain*rho*c^2/Omega = {-0.359658, -0.330273, -0.330982, -0.372997,
   -0.382777, -0.375798, -0.341584, -0.341763, -0.352812, -0.308553,
   -0.336707, -0.343647, -0.296819}
dr0*rho*c^2/(Omega*a1) = 0.345511  u1*rho*c/Omega= 1.15934

c*tt/a1 = 2.5
u*rho*c/Omega = {1.23795, 1.20181, 1.04273, 0.791454, 0.535139, 0.241807,
   -0.0281745, -0.312425, -0.612241, -0.776831, -0.980159, -1.11647,
   -1.09307}
strain*rho*c^2/Omega = {-0.341538, -0.322307, -0.329202, -0.371852,
   -0.386699, -0.373561, -0.34799, -0.343394, -0.341862, -0.331324,
   -0.34906, -0.332262, -0.298436}
dr0*rho*c^2/(Omega*a1) = 0.345792  u1*rho*c/Omega= 1.16379
DONE
```

REFERENCES

1. Waldo, Jr., G.V., "An Approximate Model for the Pressure that Develops when an Acoustic Wave Interacts with a Curved and Compliant Surface," in *Proceedings of the 65th Shock and Vibration Symposium*, Volume II, Shock and Vibration Analysis Center, Booz.Allen & Hamilton, Inc., 2231 Crystal Drive #711, Arlington, Virginia 22202, pp. 185-198 (Oct 1994).

2. Waldo, Jr., G.V., "A Virtual-Source Model for Fluid-Structure Interaction," NSWC Report CARDEROCKDIV-U-SSM-67-95/10 (Feb 1995).

3. Waldo, Jr., G.V., "Comparison of the Virtual-Source Model to Exact Calculations," in *Proceedings of the 66th Shock and Vibration Symposium*, Volume I, Shock and Vibration Analysis Center, Booz.Allen & Hamilton, Inc., 2231 Crystal Drive #711, Arlington, Virginia 22202, pp. 153-163 (Oct 1995).

4. Huang, H., "An Exact Analysis of the Transient Interaction of Acoustic Plane Waves With a Cylindrical Elastic Shell," *Journal of Applied Mechanics*, Vol. 37, pp. 1091-1099 (Dec 1970).

5. Wolfram, Stephen, *Mathematica$_R$ A System for Doing Mathematics by Computer*, Second Edition, Addison-Wesley Publishing Company, Reading, Massachusetts (1991).

6. Cole, Robert H., *Underwater Explosions*, Dover Publications, Inc., New York (1965).

7. Huang, H., "Scattering of Spherical Pressure Pulses by a Hard Cylinder," *Journal of the Acoustical Society of America*, Vol. 58, No. 2 (Aug 1975).

8. Huang, H., "Transient Interaction of Plane Acoustic Waves with a Spherical Elastic Shell," *Journal of the Acoustical Society of America*, Vol. 45, pp. 661-670 (1969).

THIS PAGE IS INTENTIONALLY BLANK.

INITIAL DISTRIBUTION

Copies	
1	DNA(SSPD) (D.Bruder and M.Giltrud)
2	ONR
	1 Code 334 (G.Main)
	1 Code 334 (R.Vogelsong)
7	NAVSEA
	1 Code 03P (R.McCarthy)
	1 Code 03P2(D.Nichols and W.Will)
	1 Code 03P3 (J.Schell)
	1 Code 03P3 (R.Bowser)
	1 Code 03P4 (D.Johansen)
	1 Code 92RC4 (D.Dozier)
	1 Code PMO (G.Becker)
1	NSWCDL CSS (Tech.Lib.)
10	NSWCIH
	1 Code 40E (Johnson)
	1 Code 460 (Harris)
	1 Code 460 (Huang)
	1 Code 460 (Mair)
	1 Code 460 (Moussouros)
	1 Code 460 (W.Reid)
	1 Code 460 (R.Barash)
	1 Code 460 (W.McDonald)
	1 Code A10 (C.McClure)
	1 Code PM3 (Kavetsky)
1	NAWC (Tech.Lib.)
1	NUWC (Tech.Lib.)
1	NRL (Tech.Lib.)
2	DTIC
1	ARPA (Tech.Lib.)

Copies	
1	Naval Postgraduate School (Y.S.Shin)
1	General Dynamics, Electric Boat Div. Dept. 442 (A.Alvarez)
1	Misovec Consulting (A.Misovec)
6	Lawrence Livermore National Lab.
	1 Code L313 (Tech.Lib.)
	1 M.Christon
	1 S.Erikson
	1 G.Goudreau
	1 D.Magnoli
	1 C.Rosenkilde
2	Weidlinger, New York
	1 R.Atkatsh
	1 K.K.Chan
1	BlazeTech (N.A.Moussa)
1	U. of Akron (M.S.HooFat)
1	Iowa State Univ. (F.J.Rizzo)
1	U. of Maryland (J.H.Duncan)
1	U. of Colorado (T.Geers)
2	Dynaflow
	1 R. Duraiswami
	1 G. Chahine
1	SUNY, Stoneybrook, NY (D.Kushner)
1	SUNY, Buffalo, NY (R.P.Shaw)
1	ETC. (T.Littlewood)

INITIAL DISTRIBUTION (CONTINUED)

Copies	
2	Tracor Hydronautics
1	V. E.Johnson
1	J.Sutton
1	Jason Associates(R. Chan)
1	Los Alamos National Lab. Tech.Lib. (Code 5000)
2	Sandia National Lab
1	Albuquerque(Tech.Lib.)
1	New Mexico(Tech.Lib.)
1	Unique Software Applications (J. DeRuntz)

CENTER DISTRIBUTION

Copies	Code	Name
2	0023	Reports Control
1	3021	TIC
1	2040	G. Everstine
1	2041	J. Slomski
1	60	G. Wacker
1	601	A. Morton
1	602	R. Rockwell
1	602	D. Martin
1	605	F. Fisch
1	605	R. Wunderlick
1	65	J. Beach
1	651	J. Sikora
1	651	M. Cheamitru
1	651	E. Devine
1	651	E. Fishlowitz
1	651	J. Rodd
1	651	R. Tacey
1	652	T. Tinley
1	652	S. Chiu
1	652	M. Costello
1	652	D. Dozier
1	652	A. Furio
1	652	D. Lesar
1	653	W. Hay
1	653	A. Dinsenbacher
1	653	L. Gifford
1	653	D. Kihl
1	654	A. Wiggs
1	654	W. Brown
1	654	J. Carlberg

CENTER DISTRIBUTION (CONTINUED)

Copies	Code	Name
1	654	W. Melton
1	654	W. Richardson
1	655	M. Critchfield
1	6551	W. Phyillaier
1	6551	H. Garala
1	6551	S. Mayes
1	6552	E. Rasmussen
1	66	M. Riley
1	662	J. Krezel
1	662	F. Costanzo
1	67	I. Hansen
1	671	B. Whang
1	671	S. Zilliacus
1	671	C. Milligan
1	671	M. Padgett
1	671	B. Tegeler
1	671	F. Rasmussen
1	671	P. Bhadra
1	671	L. Chrysostom
1	671	W. Gottwald
1	671	T. Schweich
1	671	Y. Sohn
1	672	W. Conley
1	672	D. Bond
1	672	P. Dudt
1	672	M. Hoffman
1	672	C. Nguyen
31	672	G. Waldo, Jr.
1	672	W. Gilbert
1	672	P. Manny
1	672	M. Neff
1	672	J. Ready
1	672	B. Rose
1	672	C. Stuber
1	672	S. Walter
1	673	H. Gray
1	673	H. Wolk
1	673	J. Fulton
1	673	G. Lawler
1	673	C. Tinker
1	673	D. Garrison
1	673	J. Barnum
1	673	T. Burton
1	673	P. Gaus
1	673	D. Hagar
1	673	W. Hoffman
1	673	D. Kornhauser

CENTER DISTRIBUTION (CONTINUED)

Copies	Code	Name
1	673	D. Wilson
1	673	L. Hill
1	673	C. Overman
1	673	R. Mahone
1	673	S. Poy
1	673	B. Rhee
1	673	L. Ripley
1	684	G. Gaunaurd
1	725	P. Shang

THIS PAGE IS INTENTIONALLY BLANK.